

DEC 23 1946

ARR No. 4H21

NATIONAL ADVISORY COMMITTEE FOR AERONAUTICS

WARTIME REPORT

ORIGINALLY ISSUED

August 1944 as
Advance Restricted Report 4H21

AN INVESTIGATION OF AIRCRAFT HEATERS

XIX - PERFORMANCE OF TWO FINNED-TYPE CROSSFLOW

EXHAUST GAS AND AIR HEAT EXCHANGERS

By L. M. K. Boelter, A. G. Guibert,
J. M. Rademacher, and L. J. B. Sloggy
University of California

NACA

WASHINGTON

N A C A LIBRARY
LANGLEY MEMORIAL AERONAUTICAL
LABORATORY
Langley Field, Va.

NACA WARTIME REPORTS are reprints of papers originally issued to provide rapid distribution of advance research results to an authorized group requiring them for the war effort. They were previously held under a security status but are now unclassified. Some of these reports were not technically edited. All have been reproduced without change in order to expedite general distribution.

NACA ARR No. 4H21

NATIONAL ADVISORY COMMITTEE FOR AERONAUTICS

ADVANCE RESTRICTED REPORT

AN INVESTIGATION OF AIRCRAFT HEATERS

XIX - PERFORMANCE OF TWO FINNED-TYPE CROSSFLOW

EXHAUST GAS AND AIR HEAT EXCHANGERS

By L. M. K. Boelter, A. G. Guibert,

J. M. Rademacher, and L. J. B. Sloggy

SUMMARY

Data on the thermal performance and the static pressure drop characteristics of two finned-type exhaust gas and air heat exchangers are presented. One heater was constructed of copper and stainless steel, the other was constructed entirely of an aluminum alloy. Two different shrouds were used in the tests on each exchanger.

The exhaust-gas weight rates used in the tests varied from 1800 lb/hr to 5700 lb/hr, and the ventilating-air weight rates ranged from 1000 lb/hr to 4500 lb/hr. Static pressure drop measurements were made across the exhaust-gas and ventilating-air sides of the heater under isothermal and non-isothermal conditions.

The measured thermal outputs and static pressure drops are compared with predicted magnitudes.

INTRODUCTION

The two finned-type exhaust gas and air heat exchangers were tested on the large test stand of the Mechanical Engineering Laboratories of the University of California. (See description of this test stand in reference 1.) These heaters are designed for use in the exhaust-gas streams of aircraft engines for cabin, wing, and tail-surface heating systems.

The following data were obtained:

1. Weight rates of exhaust gas and ventilating air through the respective sides of the heat exchanger.
2. Temperatures of the exhaust-gas and ventilating air at inlet and outlet of heater
3. Temperatures of the heater surfaces
4. Static pressure differences across the exhaust-gas and ventilating-air sides of the heat exchangers for isothermal and non-isothermal conditions

This report is one of a series of advance restricted reports that describe research being conducted on aircraft heat exchangers at the University of California under the sponsorship of the National Advisory Committee for Aeronautics.

SYMBOLS

- A area of heat transfer; and cross-sectional area of one fin; ft^2
- A_{cs} cross-sectional area of flow for either fluid, ft^2
- A_h cross-sectional area of flow for either fluid, measured within the heater, ft^2
- A_u area of heat transfer measured over the unfinned surfaces, ft^2
- A_1 cross-sectional area of flow taken at the inlet pressure measuring station, ft^2
- A_2 cross-sectional area of flow taken at the outlet pressure measuring station, ft^2
- c_{pa} heat capacity of air at constant pressure, $\text{Btu/lb } ^\circ\text{F}$
- c_{pg} heat capacity of exhaust gas at constant pressure, $\text{Btu/lb } ^\circ\text{F}$

- D hydraulic diameter, ft
- f_c unit thermal convective conductance (average with length), Btu/hr ft² °F
- f_{ca} unit thermal convective conductance for the ventilating air (average with length), Btu/hr ft² °F
- f_{cg} unit thermal convective conductance for the exhaust gas (average with length), Btu/hr ft² °F
- f_{cu} unit thermal convective conductance over the unfinned surfaces of the air side using the hydraulic diameter D as the significant dimension in equation (6), (average with length), Btu/hr ft² °F
- $(f_c A)_e$ "effective" thermal conductance of a finned surface, Btu/hr °F
- $(f_c A)_u$ thermal conductance of the unfinned portion of the finned surface, Btu/hr °F
- g gravitational force per unit of mass, lb/(lb sec²/ft)
- G weight rate of fluid per unit of area, lb/hr ft²
- G_u weight rate of fluid per unit of area taken at a section over the unfinned surface, lb/hr ft²
- k thermal conductivity of fin material, Btu/hr ft² (°F/ft)
- K isothermal pressure drop factor defined by the equation $\frac{\Delta P}{\gamma} = K \frac{u_m^2}{2g}$
- l significant dimension in equations for f_c along a flat plate; and the length of a fluid passage measured from the entrance, ft
- L length of a fin projecting into fluid stream, ft
- n number of fins on either side of heater
- P heat transfer perimeter of one fin (parallel to base of fin) on either side of heater, ft
- q_a measured rate of enthalpy change of ventilating air, Btu/hr or k Btu/hr (= 1000 Btu/hr)¹

¹k Btu designates kilo Btu

- q_g measured rate of enthalpy change of exhaust gas, Btu/hr or k Btu/hr (= 1000 Btu/hr)
- T_{av} arithmetic average mixed mean absolute temperature of fluid $\frac{T_1 + T_2}{2}$, $^{\circ}R$
- T_{iso} mixed-mean absolute temperature of fluid for isothermal pressure drop tests, $^{\circ}R$
- T_1 mixed-mean absolute temperature of fluid at entrance section (point 1), $^{\circ}R$
- T_2 mixed-mean absolute temperature of fluid at exit section (point 2), $^{\circ}R$
- u_m mean velocity of fluid at minimum cross-sectional area of fluid passages, ft/sec
- U over-all unit thermal conductance, Btu/hr ft² $^{\circ}F$
- (UA) over-all thermal conductance, Btu/hr $^{\circ}F$
- W weight rate of fluid, lb/hr
- W_a weight rate of ventilating air, lb/hr
- W_g weight rate of exhaust gas, lb/hr
- γ weight density of fluid, lb/ft³
- γ_1 weight density of fluid at entrance to heating section (point 1), lb/ft³
- ΔP static pressure drop, lb/ft²
- $\Delta P_a'$ static pressure drop (heater plus ducts) on ventilating-air side, inches H₂O
- $\Delta P_g'$ static pressure drop (heater plus ducts) on exhaust-gas side, inches H₂O
- ΔP_{duct} isothermal static pressure drop across inlet and outlet ducts of the air shroud or of the heater lb/ft² ($\Delta P'_{duct}$ = inches H₂O)

- ΔP_{htr} isothermal static pressure drop across the heater passages only, lb/ft² ($\Delta P'_{htr}$ = inches H₂O)
- ΔP_{iso} total isothermal static pressure drop across heater and ducts at temperature T_{iso} , lb/ft² ($\Delta P'_{iso}$ = inches H₂O)
- ξ isothermal friction factor defined by the equation
- $$\frac{\Delta P}{\gamma} = \xi \frac{l}{D} \frac{u_m^2}{2g}$$
- Δt_{mx} mean temperature difference for crossflow as defined by equation (43) of reference 2, °F
- μ viscosity of fluid, lb sec/ft²
- τ_{a1} mixed-mean temperature of ventilating air at entrance section (point 1), °F
- τ_{a2} mixed-mean temperature of ventilating air at exit section (point 2), °F
- τ_{g1} mixed-mean temperature of exhaust gas at entrance section (point 1), °F
- τ_{g2} mixed-mean temperature of exhaust gas at exit section (point 2), °F
- ϕ_x heater effectiveness for crossflow used in equation (46) of reference 2
- Re Reynolds number = $GD/3600 \mu g$

Subscripts

- a ventilating-air side
- c convective conductance
- cs cross-sectional areas
- e "effective" thermal conductances
- g exhaust-gas side
- h, htr heater

iso isothermal conditions
non-iso non-isothermal conditions
u unfinned surfaces
x crossflow

DESCRIPTION OF THE HEATERS AND OF THE TESTING PROCEDURE

The finned-type heat exchangers tested were cross-flow units with longitudinal fins in the exhaust-gas side and with short strip fins ($5/32$ in. deep) of 0.045-inch thickness on the air side. (See figures 1 to 5.)

One heater consists of a folded stainless-steel shell, the folds forming the longitudinal fins in the exhaust-gas side. Strips of copper which are attached (brazed) inside these folds form the fins on the air side. The strips are cut at approximately $5/32$ -inch intervals and the sections twisted so that the fins are parallel to the flow of air. The strip fins on the ventilating-air side are $1\frac{1}{8}$ inches long and the longitudinal fins on the exhaust-gas side are $1\frac{1}{4}$ inches long and $13\frac{1}{2}$ inches deep (along the length of the heater) with tapering ends. There are 27 fins on the exhaust-gas side and 62 fins per row (27 rows) on the air side, giving a total of 1674 fins on the air side.

The other heater consists of a folded aluminum-alloy shell, the folds again forming longitudinal fins in the exhaust-gas side. Strips of aluminum alloy are attached (welded) in the folds, cut at approximately $5/32$ -inch intervals and twisted so that they are parallel to the air stream. The fins on the air side are $1\frac{1}{4}$ inches long and those on the gas side are $1\frac{3}{16}$ inches long, the over-all depth of the gas-side fins being $13\frac{1}{4}$ inches. Since there are 26 fins on the gas side and an average of 58 fins per row (26 rows) on the air side, the total number of fins on the air side is 1508 fins.

Of the two air shrouds used on both heaters, one, referred to as UC-1, was designed to give full-crossflow characteristics; whereas the other, referred to as A-7, was designed to give "circumferential-flow" characteristics. The latter shroud is a crossflow unit with inlet and outlet

ducts which are parallel to the heat exchanger. The inlet duct contains vanes which change the direction of flow of the ventilating air, bringing it perpendicular to the heat exchanger. The shroud then guides the ventilating air around the heat exchanger for almost 360° . This type of flow will be termed circumferential flow. Diagrams and photographs of these heaters and shrouds are shown in figures 1 to 5.

Calibrated square-edge orifices were used for the measurements of the weight rates of the exhaust gas and ventilating air.

The temperatures of the exhaust gas were measured with traversing shielded thermocouples. Unshielded traversing thermocouples were employed for the measurement of the ventilating-air temperatures.¹

Temperatures of the heater surfaces were measured at several points near the entrance to the heater. Static pressure-drop measurement were made across the ventilating-air and exhaust-gas sides of the heaters. Two taps, 180° apart, were installed at each static pressure measuring station. Heat transfer and pressure drop data for the two heat exchangers using the two air shrouds are presented in tables I to X. Plots of these data as functions of the weight rates of the ventilating air and exhaust gas are presented in figures 6 to 19.

METHOD OF ANALYSIS

Heat Transfer

The thermal output of the heater was determined from the enthalpy change of the ventilating air:

$$q_a = W_a c_{p_a} (\tau_{a_2} - \tau_{a_1}) \quad (1)$$

in which c_{p_a} was evaluated at the arithmetic average ventilating-air temperature as an approximation. A plot of q_a

¹Because this thermocouple was not shielded from radiation to the relatively cooler duct walls, the measured temperatures are slightly lower than the true air temperature. A calculation shows the error to be less than 1 percent of the temperature rise of the air as it passes through the heater.

against W_a for constant values of the exhaust-gas rate (W_g) is shown in figures 6 to 9.

For the exhaust-gas side of the heater:

$$q_g = W_g c_{p_g} (\tau_{g1} - \tau_{g2}) \quad (2)$$

The over-all thermal conductance (UA) was evaluated from the expression.

$$q_a = (UA) \Delta t_{mx} \quad (3)$$

where Δt_{mx} is the mean effective temperature difference for crossflow of fluids. This term is shown graphically in reference 2 as a function of the terminal temperatures of the exhaust gas and ventilating air.

The variation of (UA) with W_a and with W_g is shown in figures 10 to 13. The thermal output of the heater for values of Δt_{mx} other than those used here may be predicted by determining (UA) at the desired weight rates from figures 10 to 13 and using these magnitudes in equation (3).¹

Predictions of the magnitudes of the over-all thermal conductances (UA) were attempted. The expression

$$(UA) = \frac{1}{\left(\frac{1}{f_c A}\right)_{ea} + \left(\frac{1}{f_c A}\right)_{eg}} \quad (4)$$

was used (reference 2, equation 47).

The terms $(f_c A)_{ea}$ and $(f_c A)_{eg}$ (the effective thermal conductances for finned surfaces in the air and gas sides of the heater, respectively) are determined from the equation [reference 2, equation (35)]:

¹This method of correction does not take cognizance of the variation of (UA) with the temperature of the fluids ($f_c \propto T_{av}^{0.296}$). For a more complete method of correction of (UA), see appendix A.

$$(f_c A)_e = n \sqrt{f_c P k A} \tanh \left[\sqrt{\frac{f_c P}{k A}} L \right] + f_{cu} A_u \quad (5)$$

where n is the number of fins, f_c the unit thermal convective conductance along the fin, P the perimeter of the fin (parallel to base of fin), k the thermal conductivity of the fin material, A the cross-sectional area of the fin, L the length of the fin (projection of fin into fluid stream), A_u the unfinned heat transfer area, and f_{cu} the unit thermal conductance over the unfinned surface.

The unit thermal convective conductances f_{ca} and f_{cg} on the ventilating-air and exhaust-gas sides were evaluated from the following equations:

(a) For the ventilating-air sides (see reference 2)

1. Unfinned surfaces

$$f_{cu_a} = 5.56 \times 10^{-4} T_{av}^{0.296} \frac{G_u^{0.8}}{D^{0.2}} \quad (6)$$

2. Finned surfaces (see reference 2)

$$f_{ca} = 9.36 \times 10^{-4} T_{av}^{0.296} \frac{G^{0.8}}{l^{0.2}} \quad (7)$$

(b) For the exhaust-gas sides: (finned and unfinned surface) (see reference 2).

$$f_{cg} = 5.56 \times 10^{-4} T_{av}^{0.296} \frac{G^{0.8}}{D^{0.2}} \left(1 + 1.1 \frac{D}{l} \right) \quad (8)$$

In these equations D is the hydraulic diameter, l is the depth of the fins in the direction of fluid flow, and G and G_u are the weight rates per unit of area corresponding to the cross-sectional areas at the sections concerned; that is, the finned and unfinned surfaces.

Equations¹ (6) and (8) are valid for the calculation of the unit thermal conductance f_c for forced convection in smooth straight ducts, but they are applied here as an approximation, inasmuch as little is known about the relation between the mechanisms of fluid and heat flow when the turbulence is of the type occasioned by large eddies. Equation¹ (7) is valid for the determination of the unit thermal conductance f_c along a flat plate in the region downstream from the point where the flow in the retarded layer along the plate has changed from laminar to turbulent flow. This equation is applicable here because with great turbulence in the stream the point of transition from a laminar to a turbulent boundary layer approaches the front edge of the plate, thus making the fraction of heat transferred through the laminar boundary layer small in comparison with that transferred through the turbulent boundary layer (which extends over the remainder of the plate).

Sample calculation. - Data taken from run no. 15, table I, for the aluminum-alloy heater using the full-crossflow (UC-1) shroud:

1. Air side

(a) Unfinned surface

The unit thermal conductance along the surface between the fin rows

$$f_{cua} = 5.56 \times 10^{-4} T_{av}^{0.296} \frac{G_u^{0.8}}{D^{0.2}}$$

$$\text{Average temperature } T_{av} = \frac{25 + 168}{2} + 460 = 591^\circ \text{ R}$$

$$\begin{aligned} \text{Weight rate per unit area } G_u &= \frac{W_a}{A_{cs}} = \frac{2650 \text{ lb/hr}}{0.325 \text{ ft}^2} \\ &= 8160 \text{ lb/hr ft}^2 \end{aligned}$$

$$\begin{aligned} \text{Hydraulic diameter } D &= 4 \times \frac{A_{cs}}{\text{wetted perimeter}} \\ &= 4 \times \frac{0.325}{5.76} = 0.226 \text{ ft} \end{aligned}$$

¹In reference 2 and also in all future reports of the series, the exponent of $T(0.296)$ has been changed to 0.3. The coefficients in the equations have been changed correspondingly.

$$f_{c_{ua}} = 5.56 \times 10^{-4} (591)^{0.296} \frac{(8160)^{0.8}}{(0.226)^{0.2}}$$

$$= 6.64 \text{ Btu/hr ft}^2 \text{ } ^\circ\text{F}$$

Unfinned heat transfer area $A_{ua} = 1.91 \text{ ft}^2$

$$\text{then } (f_c A)_{ua} = 12.7 \text{ Btu/hr } ^\circ\text{F}$$

(b) Finned surface and unfinned surface

The effective thermal conductance

$$(f_c A)_{ea} = n \sqrt{f_{ca} P k A} \tanh \left[\sqrt{\frac{f_{ca} P}{k A}} L \right] + (f_c A)_{ua}$$

The unit thermal conductance along the fins (turbulent boundary layer)

$$f_{ca} = 9.36 \times 10^{-4} T_{av}^{0.296} \frac{G^{0.8}}{l^{0.2}}$$

$$T_{av} = 591^\circ \text{ R}$$

Weight rate per unit area between fins

$$G = \frac{W_a}{A_{cs}} = \frac{2650 \text{ lb/hr}}{0.302 \text{ ft}^2} = 8770 \text{ lb/hr ft}^2$$

(cross-sectional area (A_{cs}) is taken as that between fins)

The depth of fins in direction of air flow

$$l = 0.0130 \text{ ft (5/32 in.)}$$

$$\text{so } f_{ca} = 9.36 \times 10^{-4} (591)^{0.296} \frac{(8770)^{0.8}}{(0.0130)^{0.2}}$$

$$= 21.2 \text{ Btu/hr ft}^2 \text{ } ^\circ\text{F}$$

Number of fins $n = 1508$

Perimeter of one fin $P = 0.0337$ ft

Thermal conductivity of fin material

$$k = 135 \text{ Btu/hr ft}^2 \left(\frac{^\circ\text{F}}{\text{ft}} \right)$$

Cross-sectional area of one fin $A = 4.87 \times 10^{-5}$ ft²

Length of one fin $L = 0.104$ ft

The effective thermal conductance on air side is:

$$(f_c A)_{ea} =$$

$$1508 \sqrt{21.2 \times 0.0337 \times 135 \times 4.87 \times 10^{-5}} \tanh \sqrt{\frac{21.2 \times 0.0337}{135 \times 4.87 \times 10^{-5}}} \cdot 0.104 + (f_c A)_{ua}$$

$$(f_c A)_{ea} = 82.4 + 12.7 = 95.1 \text{ Btu/hr } ^\circ\text{F}$$

2. Exhaust-gas side

The effective thermal conductance

$$(f_c A)_{eg} = n \sqrt{f_{cg} P k A} \tanh \left[\sqrt{\frac{f_{cg} P}{k A}} L \right] + f_{cg} A_u$$

Unit thermal conductance

$$f_{cg} = 5.56 \times 10^{-4} T_{av}^{0.296} \frac{G^{0.8}}{D^{0.2}} \left(1 + 1.1 \frac{D}{l} \right)$$

$$\text{Average temperature } T_{av} = \frac{968 + 879}{2} + 460 = 1380 ^\circ\text{R}$$

$$\begin{aligned} \text{Weight rate per unit area } G &= \frac{W_g}{A_{cs}} = \frac{2050 \text{ lb/hr}}{0.109 \text{ ft}^2} \\ &= 18,800 \text{ lb/hr ft}^2 \end{aligned}$$

$$\begin{aligned} \text{Hydraulic diameter } D &= 4 \times \frac{A_{cs}}{\text{wetted perimeter}} \\ &= 4 \times \frac{0.109}{6.48} = 0.0674 \text{ ft} \end{aligned}$$

Depth of fins $l = 0.940 \text{ ft}$

$$\left(1 + 1.1 \frac{D}{l}\right) = 1.08$$

$$\begin{aligned} f_{cg} &= 5.56 \times 10^{-4} (1380)^{0.296} \times \frac{(18,800)^{0.8}}{(0.0674)^{0.2}} \times 1.08 \\ &= 23.0 \text{ Btu/hr ft}^2 \text{ } ^\circ\text{F} \end{aligned}$$

Heat transfer area between fins $A_u = 1.39 \text{ ft}^2$

Number of fins $n = 26$

Heat transfer perimeter of one fin $P = 1.91 \text{ ft}$

Thermal conductivity of fin material

$$k = 155 \text{ Btu/hr ft}^2 \left(\frac{^\circ\text{F}}{\text{ft}}\right)$$

Cross-sectional area of one fin $A = 0.0123 \text{ ft}^2$

Length of fin $L = 0.099 \text{ ft}$

$$(f_{cA})_{ug} = 23.0 \times 1.39 = 3.20 \text{ Btu/hr } ^\circ\text{F}$$

$$(f_{cA})_{eg}$$

$$\begin{aligned} &= 26 \sqrt{23.0 \times 1.91 \times 15.5 \times 0.0123} \tanh \sqrt{\frac{23.0 \times 1.91}{1.55 \times 0.0123}} \times 0.099 + 23.0 \times 1.39 \\ &= 105 + 32 \\ &= 137 \text{ Btu/hr } ^\circ\text{F} \end{aligned}$$

3. Over-all thermal conductance

$$\begin{aligned} (UA) &= \frac{1}{(f_{cA})_{ea}^{-1} + (f_{cA})_{eg}^{-1}} = \frac{1}{\frac{1}{95.1} + \frac{1}{137}} \\ &= 56.3 \text{ Btu/hr } ^\circ\text{F} \end{aligned}$$

The value of (UA) obtained from the laboratory data was (see fig. 10).

$$(UA) = \frac{q_a}{\Delta t_{mx}} = \frac{46,800 \text{ Btu/hr}}{790^\circ \text{ F}} = 59.3 \text{ Btu/hr } ^\circ \text{ F}$$

where Δt_{mx} is the effective mean temperature difference for crossflow. A graphical solution Δt_{mx} , based on the terminal temperatures of the exhaust gas and ventilating air, is presented in figure 31 of reference 2.

Pressure Drop

Isothermal pressure drop

1. Ventilating-air side

The isothermal static pressure drops across the air side of the heaters were calculated in the following manner:

(a) For heaters with UC-1 shroud:

The static pressure drop in the ducts of the shroud (entrance and exit sections) was measured at different air rates (see reference 3, table VII), and then a logarithmic plot of ΔP_{ducts} against W_a was used to obtain ΔP_{ducts} at any given weight rate. This value of ΔP_{ducts} was subtracted from ΔP_{iso} , the sum of the static pressure drop across the heater alone:

$$\Delta P_{htr} = \Delta P_{iso} - \Delta P_{ducts} \quad (9)$$

A "head loss coefficient" (K) for the shroud was computed from equation (10) below, in order to evaluate the effect of the complex flow pattern which exists on the air side:

$$\frac{\Delta P_{htr}}{\gamma} = K \frac{u_m^2}{2g} \quad (10)$$

The value of K was computed (see table V) to be about 3.5 for the copper-stainless steel heater and 4.9 for the aluminum-alloy

heater (see references 3, 4, and 5 for corresponding values for other heaters).

(b) For heaters with the A-7 shroud:

The shape of this shroud was so complex that the pressure drop in the ducts alone could not be obtained readily, and consequently a head loss coefficient was calculated on the basis of the over-all static pressure drop measured across the unit (ducts, shroud, and heater). The value of K (see table V) was computed to be approximately 7.9 for the copper-stainless steel heater and 6.1 for the aluminum-alloy heater.

2. Exhaust-gas side

The isothermal static pressure drops across the exhaust-gas sides of the heaters were obtained as follows:

- (a) The static pressure drop across the inlet and outlet ducts of the gas side (approximately $1/3$ the magnitude of the over-all static pressure drop) was measured as a function of the weight rate. These values of ΔP_{ducts} were then used to obtain the static pressure drop across the heater alone, according to the equation:

$$\Delta P_{htr} = \Delta P_{iso} - \Delta P_{ducts} \quad (9)$$

where ΔP_{iso} is the over-all measured static pressure drop. The values for ΔP_{htr} are given in table VI, and those for ΔP_{iso} are plotted in figures 18 and 19.

A head loss coefficient defined to include both friction and other losses was computed on the basis of equation (10). The value of K was of the order of 0.67 for the exhaust-gas side of each heater.

An attempt was made to predict the static pressure drop across the gas side of the heater alone. The procedure followed was to compute the frictional pressure drop in the heater by use of a

suitable friction factor (f), a hydraulic diameter (D) and a mean length (l) in the Weisbach equation:

$$\frac{\Delta P}{\gamma} = f \frac{l}{D} \frac{u_m^2}{2g} \quad (11)$$

Then, the contraction and expansion losses caused by the changes in area due to the presence of fins were obtained by use of the equation (similar to equation 11):

$$\frac{\Delta P}{\gamma} = K \frac{u_m^2}{2g} \quad (12)$$

where K is a head loss coefficient the value of which was approximated by considering it as the coefficient for sudden changes in area. The sum of all these predicted pressure drops was then compared with the experimental value of ΔP_{htr} obtained according to equation (9).

For the copper-stainless steel heater the agreement between these predicted values and the experimental values obtained from equation (9) was within approximately 25 percent, and the agreement was within 10 percent in the case of the aluminum-alloy heater.

Non-isothermal pressure drop.— The non-isothermal static pressure drop across the air and gas sides of the heat exchangers was predicted from the isothermal measurements by means of equation (54), reference 2:

$$\Delta P_{non-iso} = \Delta P_{iso} \left(\frac{T_{av}}{T_{iso}} \right)^{1.13} + \left(\frac{W}{3600} \right)^2 \frac{1}{2g \gamma_1 A_h^2} \left[\left(\frac{A_h^2}{A_2^2} + 1 \right) \frac{T_2}{T_1} - \left(\frac{A_h^2}{A_1^2} + 1 \right) \right] \quad (13)$$

in which ΔP_{iso} is the measured over-all isothermal static pressure drop at the temperature T_{iso} ; T_1 and T_2 are the mixed-mean absolute temperatures of the fluid at the inlet and outlet of the heater, respectively; T_{av} is the arithmetic average of T_1 and T_2 ; W is the fluid weight rate; γ_1 is the weight density evaluated at temperature T_1 of the fluid at the inlet to the heater;

A_h is the cross-sectional area of flow within the heater; A_1 is the cross-sectional area at the inlet pressure measuring station; and A_2 is the cross-sectional area of flow at the outlet pressure measuring station.

A comparison of measured and predicted non-isothermal static pressure drops across each side of the respective heaters is presented in tables VII to X and is shown graphically in figures 14 to 19.

DISCUSSION

The results of the tests on the two finned-type heat exchangers are shown graphically. The results obtained for the copper-stainless steel heater are shown in figures 8, 9, 12, 13, 16, 17, and 19, and those for the aluminum-alloy heater are shown in figures 6, 7, 10, 11, 14, 15, and 18. Each heater was tested using the circumferential-flow shroud (designated as A-7 in the figures) and the full-crossflow shroud (designated as UC-1 in the figures).

The corresponding physical dimensions of the two heaters are approximately equal (see figure 5). The main difference is that the metals used in the construction of the heaters have dissimilar thermal conductivities. There are differences, also, in the number of fins on each heater; and, furthermore, the fins on the exhaust-gas side of the copper-stainless steel heater taper more sharply at the ends than do those of the aluminum-alloy heater (see figure 5).

The two shrouds exhibit differences not only in configuration and in flow characteristics, but also in the cross-sectional areas of flow: the area of the circumferential-flow air shroud (A-7) being 0.0985 ft^2 and that of the full cross-flow air shroud (UC-1) being 0.262 ft^2 . A further difference, of course, is that the flow path for the circumferential-flow air shroud is twice as long as that for the full-crossflow shroud.

Heat Transfer

Because of the similarity of construction of the two heaters, examination of the data should reveal what effect

the variation of the conductivity by the use of different metals and variation of the configuration of the air shrouds has upon the performance of the unit. This information can be obtained from a comparison of results taken from the data at a particular weight rate of exhaust gas and ventilating air.

<u>Heater</u>	<u>Air shroud</u>	W_g (lb/hr)	W_a (lb/hr)	(UA) (Btu/hr °F)	P_a (in. H ₂ O)	P_g (in. H ₂ O)
Copper-stainless steel	A-7	5650	2500	140	20.0	15.0
	UC-1	5650	2500	85	1.92	15.0
Aluminum-alloy	A-7	5660	2500	100	10.0	16.2
	UC-1	5660	2500	72	1.68	16.2

The foregoing table is not the correct basis for comparison because the temperatures of the exhaust gas which obtained during the tests on the copper-stainless steel heater were higher than those which obtained during the tests on the aluminum-alloy heater (1600° as against 1000° F). Because of this difference in the average fluid temperature on the gas sides, the values of (UA) should be corrected,¹ but it can be shown (see appendix A) that the correction for this difference in the average temperature of each fluid is of such a magnitude that any conclusions drawn from an inspection of the foregoing table would not be invalidated by its application.

Comparison of heaters.— The results shown in the foregoing indicate that the over-all thermal conductance (UA) of the copper-stainless steel heater using the A-7 shroud is 40 percent greater than that of the aluminum-alloy heater using the same shroud.

¹From equation (3) it is evident that the term (UA) is independent of the mean effective temperature difference Δt_{mx} . It is, however, a function of the average fluid temperature on each side of the heater inasmuch as it is a function of the unit thermal conductances on each side of the heater (the unit thermal conductance f_c varies with the 0.296 power of the absolute temperature for turbulent flow in ducts and over flat plates).

The difference in the over-all thermal conductance of the two heaters (when using the same shroud) lies mainly in the difference of the thermal conductivities of the metals used in the construction of the heaters (the thermal conductivity of copper is about 36 percent greater than that of aluminum, while the thermal conductivity of aluminum is about ten times that of stainless steel), but the differences in cross-sectional areas of fluid flow, number of fins on either side of each heater, the respective dimensions of these fins, and the difference in the average temperatures of the fluids (due to a difference in the inlet temperature of the exhaust gas) must also be considered (the unit thermal conductance f_c varies as $T_{av}^{0.296}$).

Inspection of the thermal conductances of the two heaters using the circumferential-flow (A-7) shroud, which are shown in figures 11 and 13, reveals a 40 percent increase in thermal conductance obtained with the copper-stainless steel heater. An increase of about 16 percent, as seen from the predictions, can be ascribed to the differences mentioned previously. The relative effect upon the heat transfer, of the difference in the cross-sectional areas of flow can be estimated by reference to table V, which shows a much higher pressure drop for the heater-shroud combination with the smaller cross-sectional area. Inclusion of the heat transfer by radiation and the heat transfer through the stainless steel of the fins (both neglected in the prediction; see appendix B for a discussion of the latter) would account for approximately another 14 percent of this difference.

The over-all thermal conductance of the copper-stainless steel heater using the UC-1 shroud is about 18 percent greater than that of the aluminum-alloy heater using the same shroud (see preceding table). The predictions, based on equation (5), indicate that an increase of about 14.5 percent can be ascribed to the differences in heater construction, mentioned in the preceding paragraph. Consideration of the contribution of radiant heat transfer would decrease the discrepancy, of course. When the circumferential-flow (A-7) shroud was used on the copper-stainless steel heater some of the brazing in the folds of the heater melted and drained out. Consequently, the heater performance was impaired when the heater was tested later using the full-crossflow shroud. The decrease in heat transfer due to this loss of brazing is the

reason for the apparent closer prediction of the performance of this heater when tested with the full-crossflow shroud.

Comparison of air shrouds.— Comparison of the overall thermal conductances obtained with each heater as a function of the two shrouds indicates that the circumferential-flow shroud has better thermal characteristics than the full-crossflow shroud. This is to be expected because the smaller cross-sectional area in the circumferential-flow shroud produces a higher weight rate per unit area, resulting in an increase of the unit thermal conductance (decrease of the thermal resistance) on the side with the controlling thermal resistance. For the copper-stainless steel heater, the thermal conductance obtained with the circumferential-flow shroud is about 65 percent greater than that obtained with the full-crossflow shroud. For the aluminum-alloy heater, however, the thermal conductance obtained with the circumferential-flow shroud is about 39 percent greater than that obtained with the full-crossflow shroud.¹ This increase in the thermal conductance is not the same for both heaters, mainly because, as mentioned previously, some of the brazing in the folds of the copper-stainless steel heater melted and drained out of the folds during the runs while using the circumferential-flow shroud. Thus, the performance of the heater during the runs with the full-crossflow shroud was adversely affected.

Predicted performances.— The predictions made for the copper-stainless steel heater using the A-7 shroud are on the average within 18 percent of the measured values, indicating that the method used (see appendix B) is satisfactory for the prediction of the performance of composite (binetallic) fins. The predictions for this heater using the UC-1 shroud are, on the average, within 14 percent of the measured values.

The accuracy of the predictions of the heat transfer of this heater can be increased if consideration is given to the effect of gaseous radiation and radiant exchange between

¹It should be noted, however, that the isothermal pressure drop on the air side, using the circumferential-flow air shroud, is several times that of the full-crossflow air shroud when they are used on either of the two heaters (see discussion of the pressure drop).

heater surface (about 7 percent increase in the value of (UA)) and the heat transfer through the stainless steel portion of the fins (about 7 percent increase in the value of (UA)).

The aluminum-alloy heat exchanger did not present the difficulties accompanying the analytical treatment of composite fins and consequently the predictions of the thermal performance were accomplished with greater accuracy. The average deviation of the predicted over-all conductance from the measured values was, on the average, less than 3 percent using the circumferential-flow shroud and, on the average, about 8 percent using the full-cross-flow shroud.

Isothermal Pressure Drop

Pressure drop along the gas side.— The pressure drop across the exhaust-gas side of the copper-stainless steel heater is about 60 percent of that across the exhaust-gas side of the aluminum-alloy heater. This is due, no doubt, to the greater cross-sectional area of flow of the copper-stainless steel heater. The predictions of the isothermal pressure drop were within 8 percent of the measured value in the case of the aluminum-alloy heater, and within 30 percent of the measured value in the case of the copper-stainless steel heater. The pressure loss coefficient K , defined by $\frac{\Delta P_{iso}}{\gamma} = K \frac{u_m^2}{2g}$, was about 0.68 for the aluminum-alloy heater and about 0.63 for the copper-stainless steel heater.

Pressure drop along the air side.— For the same weight rate of ventilating air, the pressure drop using the circumferential-flow shroud was about ten times that using the full-crossflow shroud in the case of the aluminum-alloy heater and about six times the latter in the case of the copper-stainless steel heater. The differences in the behavior of the two air shrouds can be ascribed to the difference in cross-sectional areas of flow, and also to the increased losses caused by the turning characteristics of the circumferential-flow shroud and to the difference in the length of the flow paths. It must be kept in mind, however, that the use of the circumferential-flow shroud made possible an increased heat transfer performance.

Non-isothermal Pressure Drop

The prediction of the non-isothermal static-pressure drop from the measured isothermal pressure drop, by means of equation (54) of reference 2, was successful in every case. (See figures 14 to 19.)

Heater Surface Temperatures

The maximum heater temperatures recorded (thermocouple located at tip of exhaust-gas side fin near gas inlet) during the runs on the aluminum-alloy heater (inlet gas temperature $\approx 1000^{\circ}$ F) were 780° F using the circumferential-flow shroud and 867° F using the full-crossflow shroud. This difference can be traced to the different flow areas of the shrouds (0.114 for the circumferential-flow shroud, 0.302 for full-crossflow shroud).

The maximum heater temperature recorded (thermocouple at tip of exhaust-gas side fin) during the runs on the copper-stainless steel heater (inlet gas temperature $\approx 1600^{\circ}$ F) was 1310° F using the full crossflow shroud. No surface temperature data were taken on this heater when using the circumferential-flow air shroud.

CONCLUSIONS

1. The over-all thermal conductance of the copper-stainless steel heater was from 20 to 40 percent greater than the value for the aluminum-alloy heater.
2. The over-all thermal conductance of the heaters, when using a circumferential-flow air shroud, was from 40 to 65 percent greater than the values obtained when using a full-crossflow air shroud.
3. The non-isothermal and isothermal static pressure drop for this circumferential flow air shroud was from six to ten times that of the full-crossflow shroud.
4. The prediction of the thermal performance was within 18 percent of the measured value for the copper-stainless heater and was within 8 percent for the aluminum-alloy heater.

University of California,
Berkeley, Calif., December 1943.

APPENDIX A

The rate of heat transfer of a certain heater at fixed fluid rates is altered when the temperature of either fluid is changed because

- (a) The heat rate is a function of the mean temperature difference (Δt_{mx}) between the two fluids and
- (b) The unit thermal conductance varies with the 0.296 power of the absolute temperature of the fluid. (See equations (6), (7), and (8).)

The correction of the heat rate necessary because of items (a) and (b) in the foregoing can be made according to equation (46) of reference 2:

$$q_a = W_a c_{p_a} (\tau_{g_1} - \tau_{a_1}) \varphi_x \quad (14)$$

where the term φ_x is the "heater effectiveness" for crossflow of fluids and is the ratio of the temperature rise of the air to the temperature difference between the gas and air at the heater inlet,

$$\varphi_x = (\tau_{a_2} - \tau_{a_1}) / (\tau_{g_1} - \tau_{a_1})$$

The heater effectiveness, φ_x , is a function of the overall thermal conductance (UA), of the fluid rates, and of the heat capacities of the fluids (see chart, fig. 34 of reference 2).

If it is desired to predict the heater output at the different inlet temperature conditions when it is known for a given set of conditions, then the foregoing corrections must be made.

The correction because of (a) alone may be obtained, as an approximation, by determining φ_x for the value of the conductance (UA) at the original temperature conditions, on the basis that (UA) and (consequently) φ_x do not change rapidly as the temperature of the fluids is varied.

The correction because of (b) can also be made using the corrected heat transfer rate from (a) to compute the new average temperatures for the ventilating-air and exhaust-gas sides. These values are used to calculate the new unit thermal conductances, on each side of the heater. On the basis of these unit thermal conductances, a new over-all conductance of the heater is calculated. Then a better approximation of ϕ_x is obtained and a new q_a computed from equation (14). Usually the change in (UA) (due to item b) is small ($f_c \propto T_{av}^{0.296}$) and the first approximation to q_a (that from the foregoing item (a) is sufficiently close.

Example:

Compute the new over-all thermal conductance for the copper-stainless steel heater using the circumferential-flow (A-7) shroud, when the inlet gas temperature is lowered from 1600° F to 970° F.

The following data are obtained from the predicted curve of figure 13:

$$W_a = 2000 \text{ lb/hr}$$

$$W_g = 5650 \text{ lb/hr}$$

$$(UA) = 110 \text{ Btu/hr } ^\circ\text{F for } \tau_{g1} = 1600^\circ \text{ F, } \tau_{a1} = 95^\circ \text{ F}$$

Desired:

$$(UA) \text{ for } \tau_{g1} = 970^\circ \text{ F, } \tau_{a1} = 95^\circ \text{ F}$$

$$\text{Postulate further that } c_{p_a} = 0.242 \text{ Btu/lb } ^\circ\text{F,}$$

$$c_{p_g} = 0.271 \text{ Btu/lb } ^\circ\text{F}$$

Obtain a new q_a , using the following equation (reference 2) which is based on inlet temperature conditions:

$$\begin{aligned} q_a &= W_a c_{p_a} (\tau_{g1} - \tau_{a1}) \phi_x \\ &= 2000 \times 0.242 \times (970 - 95) \times 0.197 \\ &= 82,700 \text{ Btu/hr} \end{aligned}$$

By use of this new q_a , the new average temperatures are obtained on the air and gas sides.

$$q_a = W_a c_{p_a} (\tau_{a_2} - \tau_{a_1}) = q_g = W_g c_{p_g} (\tau_{g_1} - \tau_{g_2})$$

$$\tau_{a_2} = \frac{q_a}{W_a c_{p_a}} + \tau_{a_1} = \frac{82700}{2000 \times 0.242} + 95 = 272^\circ \text{ F}$$

$$\tau_{g_2} = \tau_{g_1} - \frac{q_g}{W_g c_{p_g}} = 970 - \frac{82700}{5650 \times 0.271} = 916^\circ \text{ F}$$

$$\tau_a(\text{av}) = \frac{272 + 95}{2} = 184^\circ \text{ F}; \quad T_a(\text{av}) = 644^\circ \text{ R}$$

$$\tau_g(\text{av}) = \frac{970 + 916}{2} = 943^\circ \text{ F}; \quad T_g(\text{av}) = 1400^\circ \text{ R}$$

$$T_a^{0.296} = (644)^{0.296} = 6.79$$

$$T_g^{0.296} = (1400)^{0.296} = 8.55$$

Thermal conductances

Air side

1..Unfinned surface

$$f_{c_{ua}} = 5.56 \times 10^{-4} T_{av}^{0.296} \frac{G_u^{0.8}}{D^{0.2}} \quad (6)$$

$$G_u = \frac{W_a}{A_{cs}} = \frac{2000}{0.110} = 18,200 \text{ lb/hr ft}^2; \quad G_u^{0.8} = 2560$$

$$\begin{aligned} f_{c_{ua}} &= 5.56 \times 10^{-4} \times 6.79 \times \frac{2560}{0.710} \\ &= 11.4 \text{ Btu/hr ft}^2 \text{ } ^\circ\text{F} \end{aligned}$$

$$(f_{cA})_{ua} = 11.4 \times 1.68 = 19.1 \text{ Btu/hr } ^\circ\text{F}$$

2. Finned surface

$$f_{ca} = 9.36 \times 10^{-4} T_a^{0.296} \frac{G_a^{0.8}}{l^{0.2}} \quad (7)$$

$$G_a = \frac{W_a}{A_{cs}} = \frac{2000}{0.0985} = 20,300 \text{ lb/hr ft}^2; G_a^{0.8} = 2800$$

$$f_{ca} = 9.36 \times 10^{-4} 6.79 \frac{2800}{0.419} = 42.5 \text{ Btu/hr ft}^2 \text{ } ^\circ\text{F}$$

3. Equivalent thermal conductance on air side

$$(f_c A)_{ea} = n \sqrt{f_c P k A} \tanh \sqrt{\frac{f_c P}{k A}} L + (f_c A)_{ua}$$

$$= 1674 \sqrt{42.5 \times 0.0336 \times 210 \times 4.87 \times 10^{-5}} \tanh \sqrt{\frac{42.5 \times 0.0336}{210 \times 4.87 \times 10^{-5}}} \times 0.0937 + 18.9$$

$$(f_c A)_{ea} = 162 + 19 = 181 \text{ Btu/hr } ^\circ\text{F}$$

$$\frac{1}{(f_c A)_{ea}} = 0.00552$$

Gas side

$$f_{cg} = 5.56 \times 10^{-4} T_g^{0.296} \frac{G_g^{0.8}}{D_g^{0.2}} (1 + 1.1 \frac{D_g}{l}) \quad (8)$$

$$f_{cg} = 5.56 \times 10^{-4} \times 8.55 \times \frac{4750}{0.601} (1.086)$$

$$= 40.8 \text{ Btu/hr ft}^2 \text{ } ^\circ\text{F}$$

1. Unfinned surface

$$(f_c A)_{ug} = 40.8 \times 1.43 = 58.4 \text{ Btu/hr } ^\circ\text{F}$$

2. Finned surface and unfinned surface

$$(f_c A)_{eg} = n \sqrt{f_c P k A} \tanh \sqrt{\frac{f_c P}{k A}} L + (f_c A)_{ug}$$

$$= 27 \sqrt{40.8 \times 2.06 \times 210 \times 0.00383} \tanh \sqrt{\frac{40.8 \times 2.06}{210 \times 0.00383}} \times 0.1043 + 58$$

$$= (175 + 58) \text{ Btu/hr } ^\circ\text{F}$$

3. Equivalent $(f_c A)$ on gas side

$$(f_c A)_{eg} = 175 + 58 = 233 \text{ Btu/hr } ^\circ\text{F}$$

$$\frac{1}{(f_c A)_{eg}} = 0.00429$$

Over-all thermal conductance:

$$(UA) = \frac{1}{\left(\frac{1}{f_c A}\right)_{ea} + \left(\frac{1}{f_c A}\right)_{eg}} = \frac{1}{0.00552 + 0.00429}$$

$$= 102 \text{ Btu/hr } ^\circ\text{F}$$

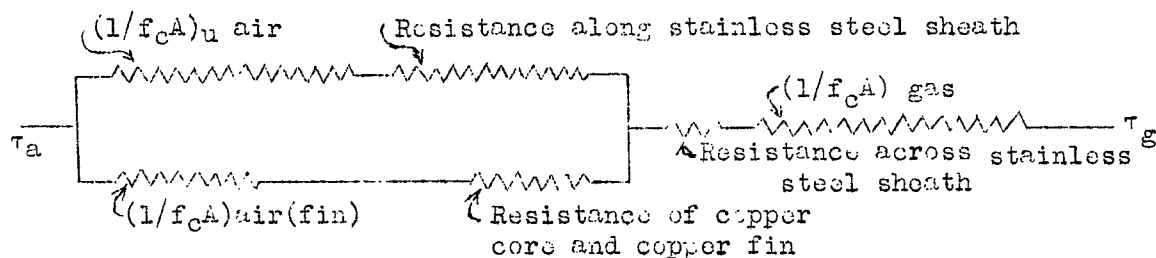
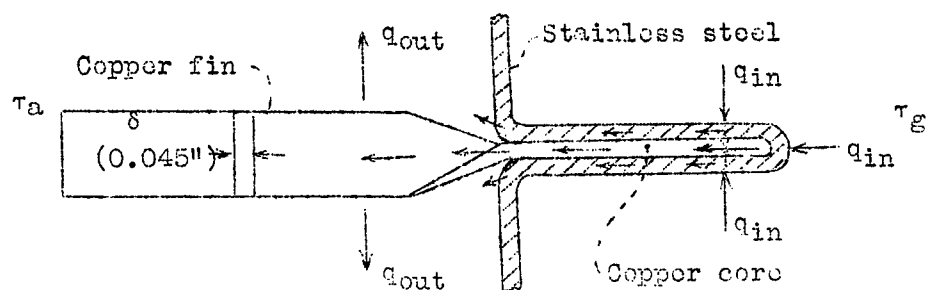
Since the (UA) obtained is so close to that which was postulated in making the calculation ($UA = 110 \text{ Btu/hr } ^\circ\text{F}$) the first approximation is within the limit of accuracy and will suffice.

Hence, it can be said that a change in the average temperature of the exhaust-gases has little effect upon the over-all-thermal conductance (only 7 percent in this case). Consequently, if the thermal performance of a heat exchanger is known for some certain inlet temperature conditions, an estimate of the thermal performance at some other inlet temperature conditions can be obtained, without greatly impairing the accuracy of calculation, by using equation (14) considering only the new inlet temperature conditions. Such procedure neglects any change in φ_x which might be caused by the dependence of (UA) upon the average temperature of the fluids flowing through the heat exchanger.

APPENDIX B

Predictions of the performance of the copper-stainless steel heater were made by substitution of "equivalent copper fins" for the composite fins on the exhaust-gas side. This idealization is permissible if the following system is visualized (see sketch); Heat flows from the gas through a "fluid thermal resistance" into the stainless steel of the fin. In the stainless steel the heat (considering two-

dimensional flow only) will flow into the base of the fin and also into the copper core of the fin. The heat flowing into the copper core will flow to the base of the gas-side fin and then into the fins on the air side.



Thermal circuit of above fins (idealized)

If this system is considered as a group of resistances in series and in parallel, it will give, as a first idealization, for flow to the copper core the fluid thermal resistance of the exhaust gas in series with the resistance of the stainless steel. Since the fluid thermal resistance of the exhaust gas is much greater than that of the stainless steel, and these resistances are in series, the latter resistance may be neglected in calculating the heat flow to the center of the fin. For flow to the base of the fin, the resistance of the stainless steel is in parallel with

the resistance of the copper. Because the sum of the resistance of the copper core and copper fin and the fluid thermal resistance of the ventilating-air side is much smaller than the sum of the resistance along the stainless steel sheath and the fluid thermal resistance of the unfinned portion of the air side of the heater, and since these sets of resistances are in parallel, the larger resistance can be neglected, as an approximation, in making the computations of the heat flow through these composite fins. Hence, it may be said that the composite fin of stainless steel ($k = 15 \text{ Btu/hr ft}^2 (\text{°F/ft})$) and copper ($k = 210 \text{ Btu/hr ft}^2 (\text{°F/ft})$) may be considered as an "equivalent" fin of copper alone.

The equation for the heat transfer from the finned surface is valid for fins of finite length with insulated ends. This equation can be used because the heat loss from the ends of the air side fins is small in comparison with that through the sides.

In the equation for the heat transfer from the finned surface, the unit thermal conductance over this "equivalent copper" fin would be the same as that over the stainless steel surface, but the perimeter, cross-sectional area and thermal conductivity would be those of the copper alone.

REFERENCES

1. Boelter, L. M. K., Miller, M. A., Sharp, W. E., Morrin, E. H., Iversen, H. W., and Mason, W. E.: An Investigation of Aircraft Heaters. IX - Measured and Predicted Performance of Two Exhaust Gas-Air Heat Exchangers and an Apparatus for Evaluating Exhaust Gas-Air Heat Exchangers. NACA ARR, March 1943.
2. Boelter, L. M. K., Martinelli, R. C., Romie, F. E., and Morrin, E. H.: An Investigation of Aircraft Heaters. XVIII - A Design Manual for Exhaust Gas and Air Heat Exchangers. NACA ARR No. 5A06, 1945.

3. Boelter, L. M. K., Miller, M. A., Sharp, W. H., and Morrin, E. H.: An Investigation of Aircraft Heaters. XI - Measured and Predicted Performance of a Slotted-Fin Exhaust Gas and Air Heat Exchanger. NACA ARR No. 3D16, April 1943.
4. Boelter, L. M. K., Dennison, H. G., Guibert, A. G., and Morrin, E. H.: An Investigation of Aircraft Heaters. XII - Performance of a Formed-Plate Cross-flow Exhaust Gas and Air Heat Exchanger. NACA ARR No. 3E10, May 1943.
5. Boelter, L. M. K., Guibert, A. G., Miller, M. A., and Morrin, E. H.: An Investigation of Aircraft Heaters. XIII - Performance of Corrugated and Noncorrugated Fluted Type Exhaust Gas-Air Heat Exchangers. NACA ARR No. 3H26, Aug. 1943.

TABLE I — EXPERIMENTAL RESULTS ON FINNED-TYPE HEATER
ALUMINUM-ALLOY UC-I SHROUD

Run No.	AIR SIDE						EXHAUST-GAS SIDE						$\frac{q_g}{q_a}$	HEATER TEMPS.					OVERALL PERFORMANCE	
	T_{a1}	T_{a2}	ΔT_a	W_a	ΔP_a	q_a	T_{g1}	T_{g2}	ΔT_g	W_g	ΔP_g	q_g		Shell	Gas Side Fin Tip	Gas Side Fin Tip	Gas Side Fin Tip	Gas Side Fin Tip	ΔT_{ex}	(UA)
	$^{\circ}F$	$^{\circ}F$	$^{\circ}F$	$\frac{lb.}{hr.}$	$\frac{Inches}{H_2O}$	$\frac{KBtu.}{hr.}$	$^{\circ}F$	$^{\circ}F$	$^{\circ}F$	$\frac{lb.}{hr.}$	$\frac{Inches}{H_2O}$	$\frac{KBtu.}{hr.}$		$^{\circ}F$	$^{\circ}F$	$^{\circ}F$	$^{\circ}F$	$^{\circ}F$	$^{\circ}F$	$\frac{BTU.}{hr. ^{\circ}F}$
11	92	206	114	2230	1.34	61.4	1065	1006	59	5640	16.8	86.8	1.41	815	845	867	870	875	887	69.3
9	88	174	86	3160	2.48	65.7	994	947	47	5770	17.1	70.8	1.08	735	760	790	793	815	835	78.7
10	88	158	70	4510	4.80	76.1	998	947	51	5680	16.3	75.6	0.99	—	675	—	767	775	850	89.6
12	95	249	154	1070	0.30	39.9	989	939	50	3880	7.60	50.6	1.27	793	815	830	835	840	790	50.5
13	92	214	122	1780	0.83	52.6	989	939	50	3900	7.60	50.8	0.97	730	777	795	795	805	803	65.5
14	95	185	90	2690	1.76	58.6	994	935	59	3900	7.52	60.0	1.02	712	740	765	765	770	725	71.0
17	92	216	124	1040	0.36	31.2	943	871	72	2050	2.05	38.5	1.23	692	712	725	725	730	750	41.6
16	96	189	93	1750	0.86	39.4	952	867	85	2050	2.04	45.4	1.15	640	665	680	680	690	765	57.5
15	95	168	73	2650	1.72	46.8	968	879	89	2050	2.04	47.6	1.02	600	625	645	645	655	790	59.3

TABLE II — EXPERIMENTAL RESULTS ON FINNED-TYPE HEATER
ALUMINUM-ALLOY A-7 SHROUD

Run No.	AIR SIDE						EXHAUST-GAS SIDE						q_g/ρ_a	HEATER TEMPS.			OVERALL PERFORMANCE	
	T_{a1} °F	T_{a2} °F	ΔT_a °F	W_a $\frac{Lb}{Hr}$	$\Delta P_a'$ $\frac{Inches}{H_2O}$	q_a $\frac{KBtu}{Hr}$	T_{g1} °F	T_{g2} °F	ΔT_g °F	W_g $\frac{Lb}{Hr}$	$\Delta P_g'$ $\frac{Inches}{H_2O}$	q_g $\frac{KBtu}{Hr}$		Shell °F	Gas Side Fin Tip °F	Gas Side Fin Tip °F	$\Delta T_{m,x}$ °F	(UA) $\frac{Btu}{Hr \cdot ^\circ F}$
12	94	260	166	1000	1.92	40.0	960	875	85	1810	1.65	40.2	1.00	600	660	695	740	54.1
13	94	204	110	1870	5.87	496	930	854	76	1810	1.60	36.0	0.73	510	590	620	740	67.0
14	94	176	82	2660	11.4	52.6	926	837	89	1810	1.58	42.2	0.80	460	550	575	746	70.5
9	93	265	172	1380	3.51	57.5	1002	930	72	3440	6.01	64.8	1.13	660	740	770	780	73.7
10	92	234	142	1890	6.19	65.0	998	926	72	3450	5.97	65.1	1.00	610	705	740	790	82.2
11	91	205	114	2660	11.0	73.2	1007	922	85	3450	5.95	76.9	1.05	560	675	705	810	90.5
23	93	233	140	2280	8.71	77.2	977	930	47	5760	16.6	70.4	0.91	630	760	780	788	98.0
24	93	194	101	3950	23.1	96.6	981	913	68	5690	16.0	101	1.04	—	—	—	800	118

TABLE III — EXPERIMENTAL RESULTS ON FINNED-TYPE HEATER
COPPER-STAINLESS STEEL UC-1 SHROUD

Run No.	AIR SIDE						EXHAUST-GAS SIDE						$q_{g/2}$	HEATER TEMPS.			OVERALL PERFORMANCE	
	T_{a1} °F	T_{a2} °F	ΔT_a °F	W_a $\frac{Lb}{Hr}$	ΔP_a $\frac{Inches}{H_2O}$	q_a $\frac{K.Btu.}{Hr.}$	T_{g1} °F	T_{g2} °F	ΔT_g °F	W_g $\frac{Lb}{Hr}$	ΔP_g $\frac{Inches}{H_2O}$	q_g $\frac{K.Btu.}{Hr.}$		T_{g1} °F			Δt_{mx} °F	(UA) $\frac{Btu.}{Hr. °F}$
3	95	287	192	2300	1.65	107	1494	1442	52	5690	14.5	80.1	0.75	1300	-	-	1280	84
4	97	257	160	3030	2.69	117	1525	1455	70	5620	14.5	106	0.91	1260	-	-	1320	89
5	87	239	152	3590	3.51	132	1530	1451	79	5640	14.6	121	0.91	1245	-	-	1330	99
7	92	381	289	1030	0.40	72.0	1547	1534	43	2780	3.60	32.4	0.45	1310	-	-	1250	58
8	95	312	217	1670	0.92	87.6	1578	1551	27	2780	3.62	20.3	0.23	1260	-	-	1320	66
9	92	253	161	2660	2.08	104	1556	1460	96	2800	3.61	72.8	0.71	1200	-	-	1320	78
12	92	372	280	1000	0.44	67.7	1547	1446	101	2490	2.94	69.1	1.02	1285	-	-	1310	52
11	92	300	208	1680	0.91	84.5	1538	1442	96	2510	2.84	65.3	0.77	1210	-	-	1290	66
10	93	243	150	2660	2.06	96.4	1538	1420	118	2510	2.85	73.5	0.76	1140	-	-	1290	75

TABLE IV — EXPERIMENTAL RESULTS ON FINNED-TYPE HEATER

COPPER-STAINLESS STEEL

A-7 SHROUD

Run No	AIR SIDE						EXHAUST GAS SIDE							HEATER TEMPS.		OVERALL PERF.	
	T_{a_1}	T_{a_2}	ΔT_a	W_a	ΔP_a	q_a	T_{g_1}	T_{g_2}	ΔT_g	W_g	ΔP_g	q_g	$\frac{q_a}{q_g}$			$\Delta T_{m,x}$	(UA)
	°F	°F	°F	$\frac{lb}{hr}$	$\frac{Inches}{H_2O}$	$\frac{KBtu}{hr}$	°F	°F	°F	$\frac{lb}{hr}$	$\frac{Inches}{H_2O}$	$\frac{KBtu}{hr}$		°F	°F	°F	$\frac{Btu}{hr °F}$
1	105	418	313	2130	11.7	161	1569	1458	111	4120	7.83	124	0.77	HEATER TEMPS. NOT RECORDED		1260	128
2	108	344	236	2940	22.6	168	1564	1433	131	4120	7.82	146	0.87			1280	130
3	108	437	329	2200	13.1	175	1582	1482	100	5650	15.1	153	0.87			1270	138
4a	107	373	266	2840	23.7	183	1582	1473	109	5650	15.0	167	0.91			1290	142
20	109	449	340	1400	6.78	115	1573	1442	131	2700	3.35	95.8	0.83			1250	91.4
21	109	395	286	1870	11.8	129	1573	1447	126	2700	3.34	92.0	0.71			1260	103
23	113	558	445	990	3.38	107	1591	1477	114	2690	3.37	83.1	0.78			1200	88.8
22	109	329	220	2630	22.3	140	1582	1428	154	2700	3.32	113	0.80			1290	109
24	113	528	415	990	3.30	99.6	1569	1455	114	1950	1.86	60.2	0.60			1180	84.4
25	111	431	320	1390	6.81	108	1569	1438	131	1970	1.83	69.9	0.65			1230	87.6
27	109	305	196	2630	22.2	124	1556	1398	158	1970	1.82	84.4	0.68			1270	98.0

TABLE V - ISOTHERMAL PRESSURE DROP DATA

Ventilating-Air Side						
Run No.	W lb/hr	G lb/hr ft ²	$\Delta P'_{iso}$ in. H ₂ O	$= \Delta P'_{duct} + \Delta P'_{htr}$ in. H ₂ O	$\Delta P'_{htr}$ in. H ₂ O	K
Copper-Stainless Steel Heater						
1. Full-crossflow (UC-1) shroud.						
12	1000	3820	0.25	0.08	0.17	3.6 ^a
9	2650	10,100	1.38	0.20	1.18	3.5
2	4120	15,700	3.41	0.56	2.85	3.5
2. Circumferential-flow (A-7) shroud						
-	1000	10,100	2.70	-	-	7.8 ^b
-	1500	15,200	6.10	-	-	7.9
-	2500	25,400	17.3	-	-	8.0
Aluminum-Alloy Heater						
1. Full-crossflow (UC-1) shroud						
4	1040	3,440	0.28	0.09	0.19	4.9 ^a
1	2640	8,740	1.50	0.22	0.22	5.1
6	4200	13,900	3.63	0.58	0.58	4.8
2. Circumferential-flow (A-7) shroud						
4	1030	9,030	1.77	-	-	6.8 ^b
18	2270	19,900	7.65	-	-	6.1
15	4180	36,600	23.9	-	-	5.6

a) K defined by $\frac{\Delta P_{htr}}{\gamma} = K \frac{u_m^2}{2g}$, ft.

b) K defined by $\frac{\Delta P_{iso}}{\gamma} = K \frac{u_m^2}{2g}$, ft

TABLE VI - ISOTHERMAL PRESSURE DROP DATA

Exhaust-Gas Side								
Run No.	W lb/hr	G lb/hr ft ²	$\Delta P'_{iso}$ in. H ₂ O	$\Delta P'_{duct}$ in. H ₂ O	$\Delta P'_{htr}$ meas. in. H ₂ O	$\Delta P'_{htr}$ pred. in. H ₂ O	Re	K
Copper-Stainless Steel Heater								
-	1500	10,600	0.28 ^a	0.06	0.22	0.16	18,700	0.66
-	3000	21,100	1.07	0.24	0.83	0.59	37,400	0.63
-	6000	42,200	4.13	0.97	3.16	2.10	74,800	0.60
Aluminum-Alloy Heater								
8	1660	15,200	0.59	0.08	0.51	0.48	22,100	0.77
6	3300	30,500	2.12	0.30	1.82	1.68	44,000	0.69
3	5130	47,000	4.90	0.71	4.19	3.93	68,400	0.66
1	9170	84,200	15.6	2.30	13.3	11.8	122,000	0.66

a) For copper-stainless steel heater, values of $\Delta P'_{iso}$ were interpolated from plot, figure 19.

b) For method of predicting $\Delta P'_{htr}$, see text.

c) K defined by $\frac{\Delta P_{htr}}{\gamma} = K \frac{u_m^2}{2g} = K \frac{W^2}{2g(A \cdot \gamma \cdot 3600)^2}$

TABLE VII - NON-ISOTHERMAL PRESSURE DROP DATA

Aluminum-Alloy Heater								
Full-crossflow (UC-1) shroud								
Run No.	W lb/hr	G lb/hr ft ²	T ₁ °R	T ₂ °R	T _{ave} °R	$\Delta P'_{iso}$ ^a in. H ₂ O	$\Delta P'_{non-iso}$ ^b pred. in. H ₂ O	$\Delta P'_{non-iso}$ meas. in. H ₂ O
Exhaust-Gas Side								
17	2050	18,800	1403	1331	1367	0.86	2.20	2.05
14	3900	35,800	1454	1395	1425	3.00	8.22	7.52
10	5680	52,000	1458	1407	1433	6.00	16.7	16.3
Ventilating-Air Side								
13	1780	5,900	552	674	616	0.72	0.95	0.83
15	2650	8,800	555	628	591	1.47	1.77	1.72
9	3160	10,500	548	634	591	2.05	2.53	2.48

a) Values of $\Delta P'_{iso}$ were interpolated from plot of $\Delta P'_{iso}$ vs. W_a of figure 14.

b) Prediction based on equation (13).

TABLE VIII - NON-ISOTHERMAL PRESSURE DROP

Aluminum-Alloy Heater								
Circumferential-flow (A-7) shroud								
Run No.	W lb/hr	G lb/hr ft ²	T ₁ °R	T ₂ °R	T _{ave} °R	$\Delta P'_{iso}$ ^a in. H ₂ O	$\Delta P'_{non-iso}$ ^b pred. in. H ₂ O	$\Delta P'_{non-iso}$ meas. in. H ₂ O
Exhaust-Gas Side								
14	1810	16,610	1386	1297	1342	0.69	1.71	1.58
11	3460	31,800	1467	1382	1425	2.47	6.34	5.95
23	5760	52,800	1437	1390	1314	6.20	17.0	16.6
Ventilating-Air Side								
12	1000	8,770	1014	1180	1097	1.70	2.10	1.92
13	1880	16,500	1014	1123	1069	5.40	6.24	5.87
14	2660	23,300	1014	1096	1055	10.5	11.7	11.4

a) Values of $\Delta P'_{iso}$ were interpolated from plot of $\Delta P'_{iso}$ vs. W_a of figure 15.

b) Prediction based on equation (13).

TABLE IX - NON-ISOTHERMAL PRESSURE DROP DATA

Copper-Stainless Steel Heater								
Full-crossflow (UC-1) shroud								
Run No.	W lb/hr	G lb/hr ft ²	T ₁ °R	T ₂ °R	T _{ave} °R	$\Delta P'_{iso}$ ^a in.H ₂ O	$\Delta P'_{non-iso}$ ^b pred. in.H ₂ O	$\Delta P'_{non-iso}$ meas. in.H ₂ O
Exhaust-Gas Side								
3	5690	40,100	1954	1902	1928	3.94	15.5	14.5
9	2800	19,700	2016	1920	1968	0.99	3.88	3.61
12	2490	17,600	2006	1906	1956	0.79	3.06	2.94
Ventilating-Air Side								
7	1030	3,920	552	841	696	0.25	0.45	0.40
11	1680	6,390	552	760	656	0.61	0.97	0.91
10	2660	10,190	553	703	628	1.42	2.05	2.06

a) Values of $\Delta P'_{iso}$ were interpolated from plot of $\Delta P'_{iso}$ vs. W_a of figure 16.

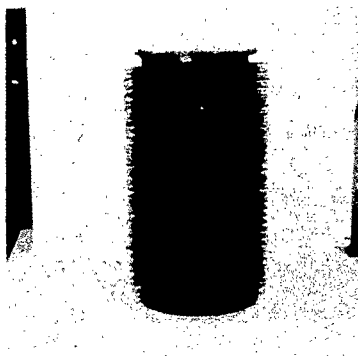
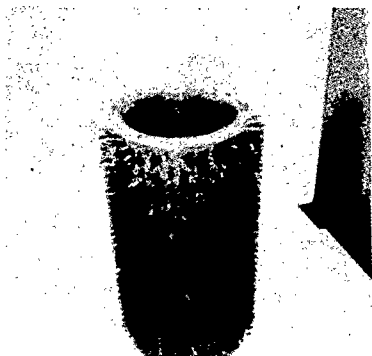
b) Prediction based on equation (13).

TABLE X - NON-ISOTHERMAL PRESSURE DROP DATA

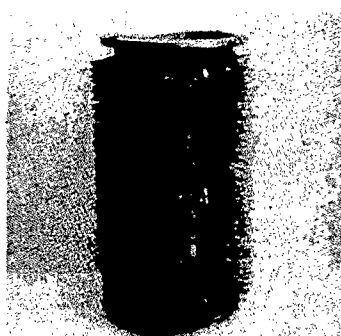
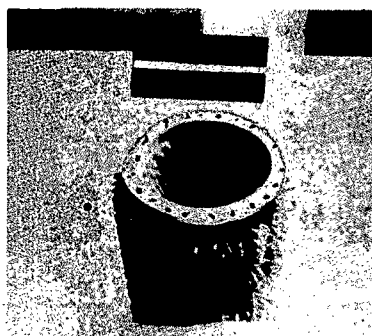
Copper-Stainless Steel Heater								
Circumferential-flow (A-7) shroud								
Run No.	W lb/hr	G lb/hr ft ²	T ₁ °R	T ₂ °R	T _{ave} °R	$\Delta P'_{iso}$ ^a in.H ₂ O	$\Delta P'_{non-iso}$ ^b pred. in.H ₂ O	$\Delta P'_{non-iso}$ meas. in.H ₂ O
Exhaust-Gas Side								
27	1970	13,900	2016	1858	1937	0.49	1.78	1.82
20	2700	19,000	2033	1902	1967	0.90	3.38	3.35
1	4120	29,000	2025	1918	1971	2.00	7.62	7.83
3	5650	39,800	2042	1942	1992	3.65	14.2	15.1
Ventilating-Air Side								
24	990	10,100	573	988	780	2.65	4.20	3.38
20	1390	14,100	569	909	739	5.20	7.60	6.78
21	1870	19,000	569	855	712	9.45	13.3	11.8
22	2630	26,700	569	789	679	19.0	24.6	22.3

a) Values of $\Delta P'_{iso}$ interpolated from plot of $\Delta P'_{iso}$ vs. W_a of figure 17.

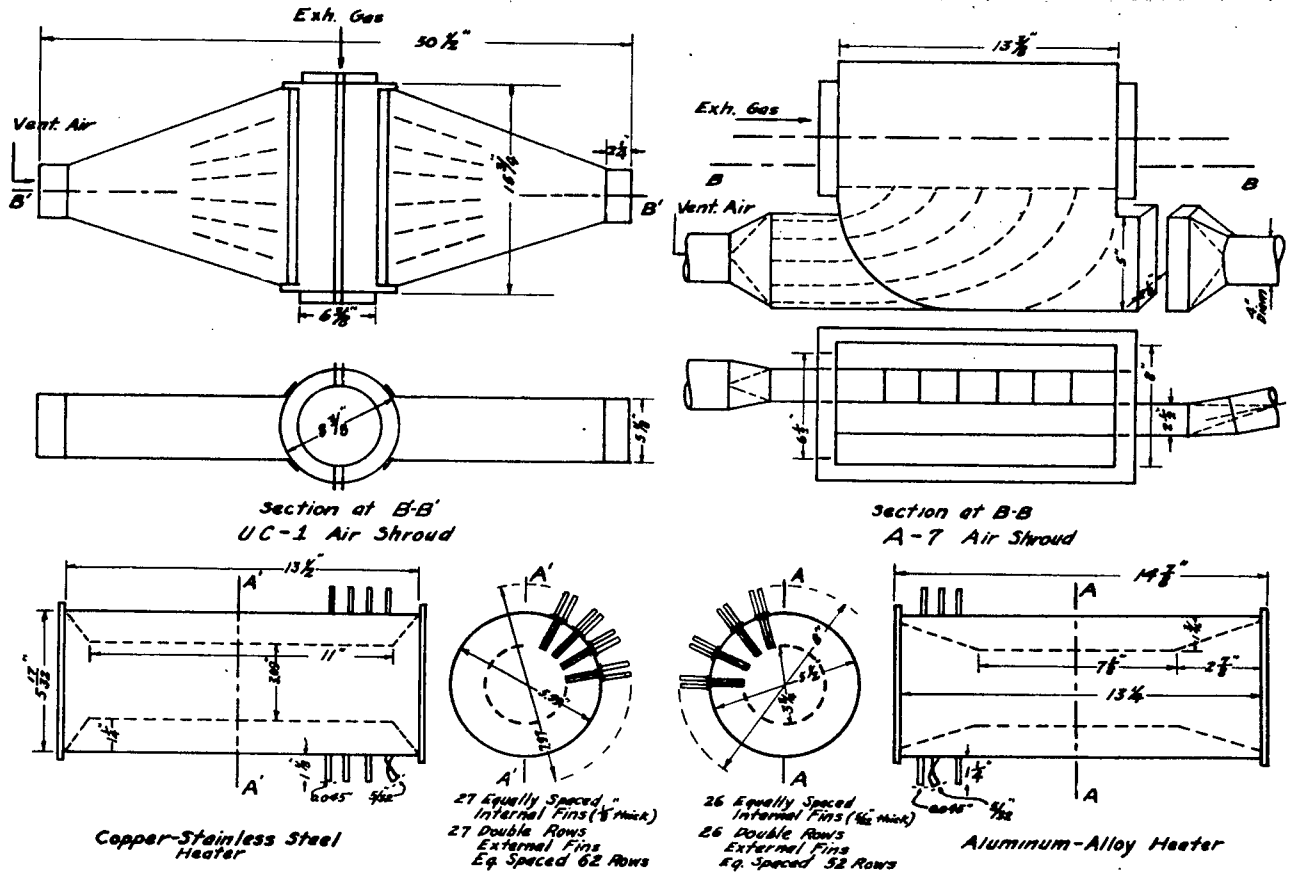
b) Prediction based on equation (13).



Figures 1 and 2.- Photographs of copper-stainless steel heater.



Figures 3 and 4.- Photographs of aluminum-alloy heater.



COPPER-STAINLESS STEEL HEATER				ALUMINUM-ALLOY HEATER			
Weight	Air Side		Gas Side	Weight	Air Side		Gas Side
Lbs.	UC-1	A-7		Lbs.	UC-1	A-7	
24.5	(Areas Taken Along Row of Fins)			10.0	(Areas Taken Along Row of Fins)		
Cross-sectional Area Ft. ²	0.262	0.0985	0.142	0.302	0.114	0.109	
Total Wetted Perimeter Ft.	17.3	8.23	7.08	17.8	8.49	6.48	
Hydraulic Diameter Ft.	0.0727	0.0574	0.0804	0.0831	0.0645	0.0674	

Fig. 5 - Schematic Diagram of Finned Type Heat Exchangers and A-7 and UC-1 Shrouds.

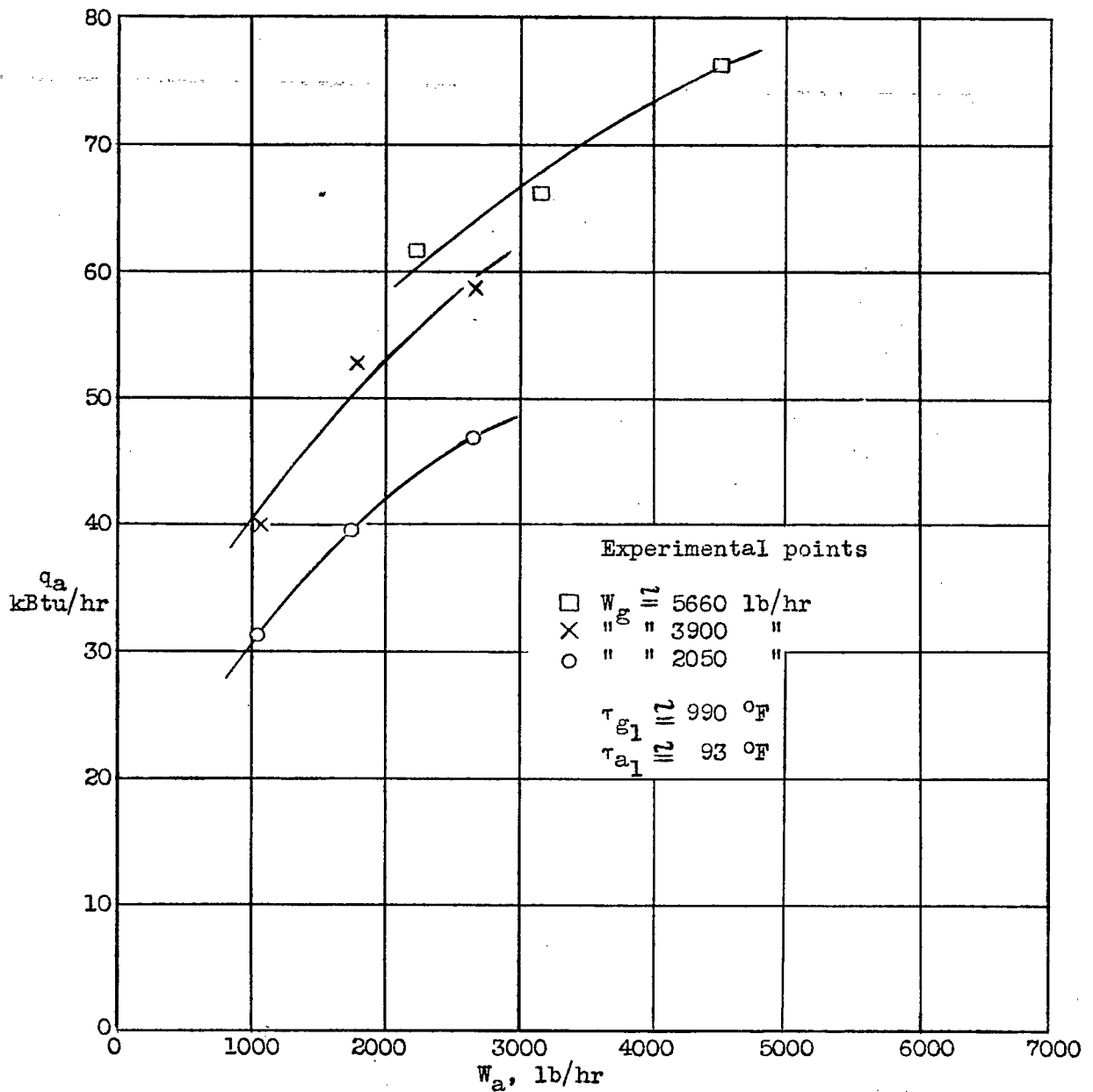


Figure 6.- Thermal output of the aluminum-alloy finned-type heater, using UC-1 shroud, as a function of ventilating air rate.

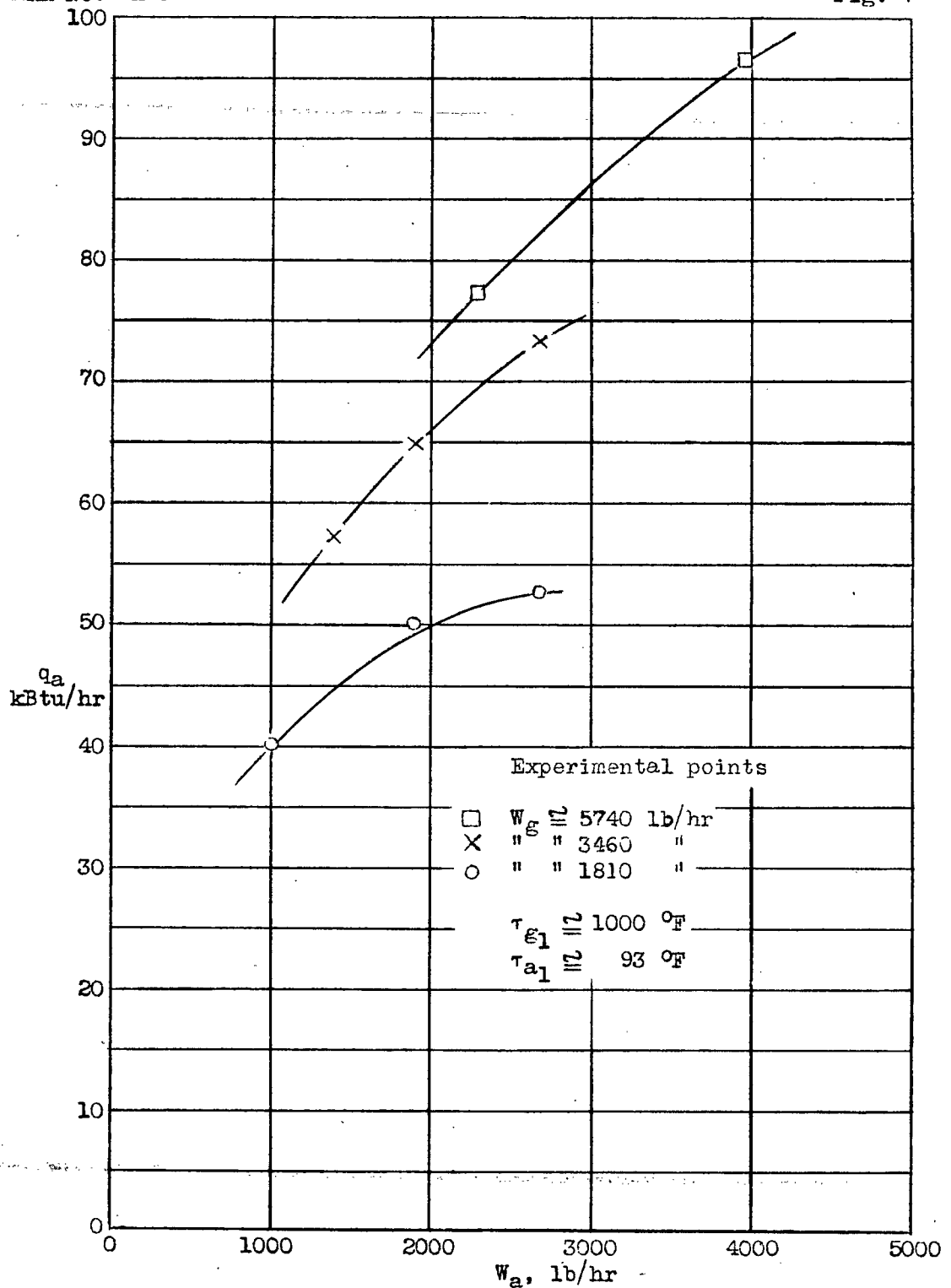


Figure 7.- Thermal output of the aluminum-alloy finned-type heater, using A-7 shroud, as a function of ventilating air rate.

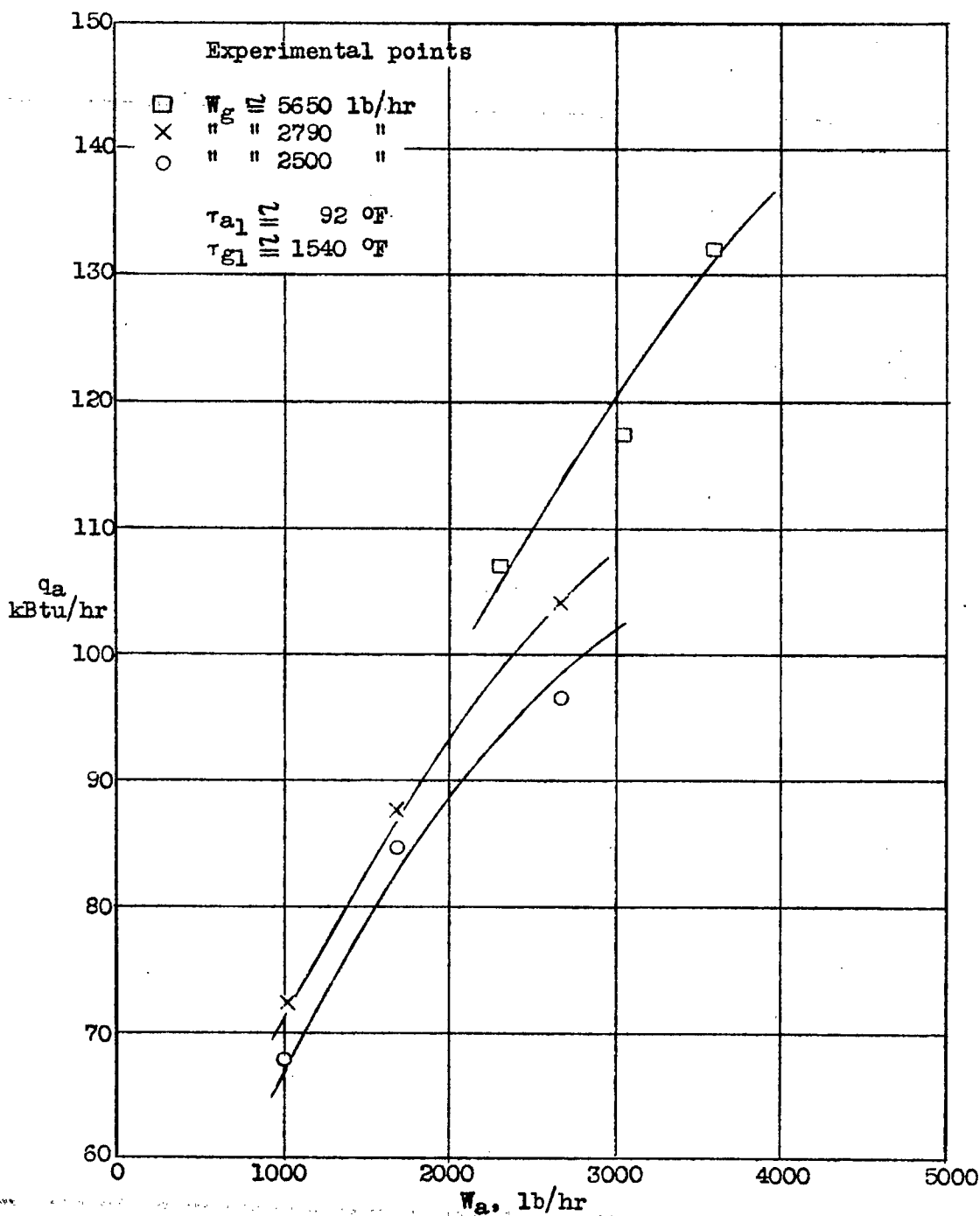


Figure 8.- Thermal output of the copper-stainless steel finned-type heater, using UC-1 shroud, as a function of ventilating air rate.

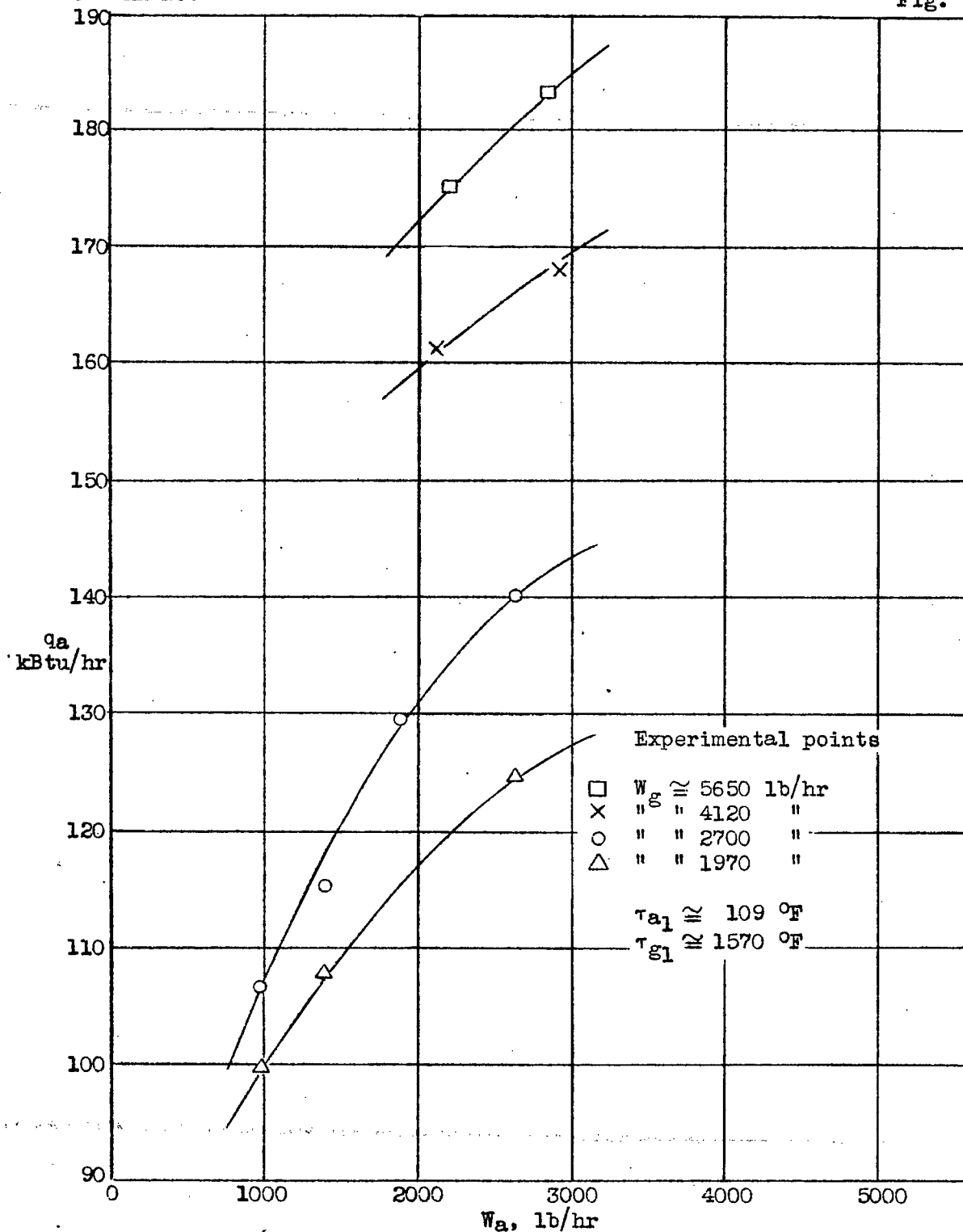


Figure 9.- Thermal output of the copper-stainless steel finned-type heater, using A-7 shroud, as a function of ventilating air rate.

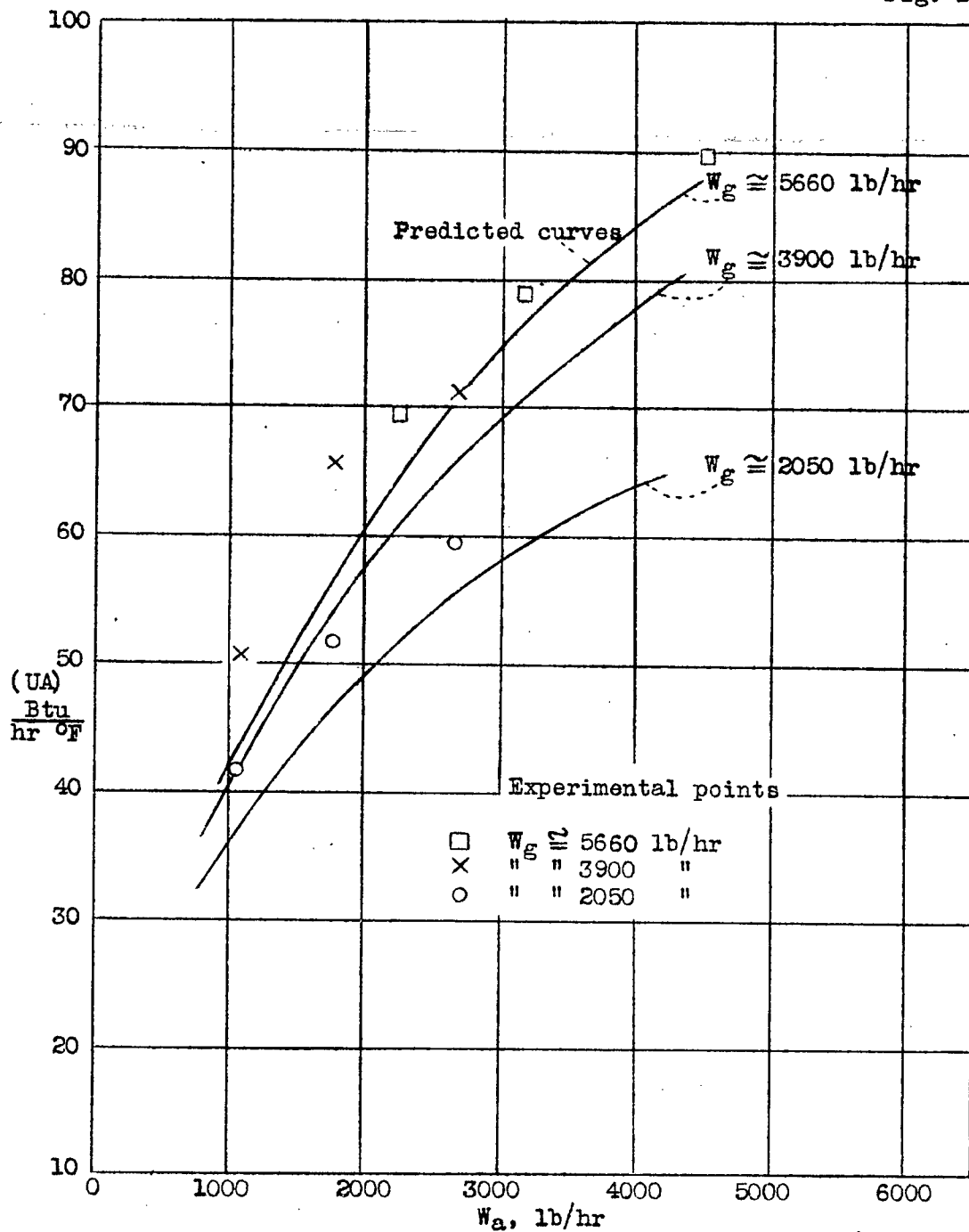


Figure 10.- Overall thermal conductance of the aluminum-alloy finned-type heater, using UC-1 shroud, as a function of ventilating air rate.

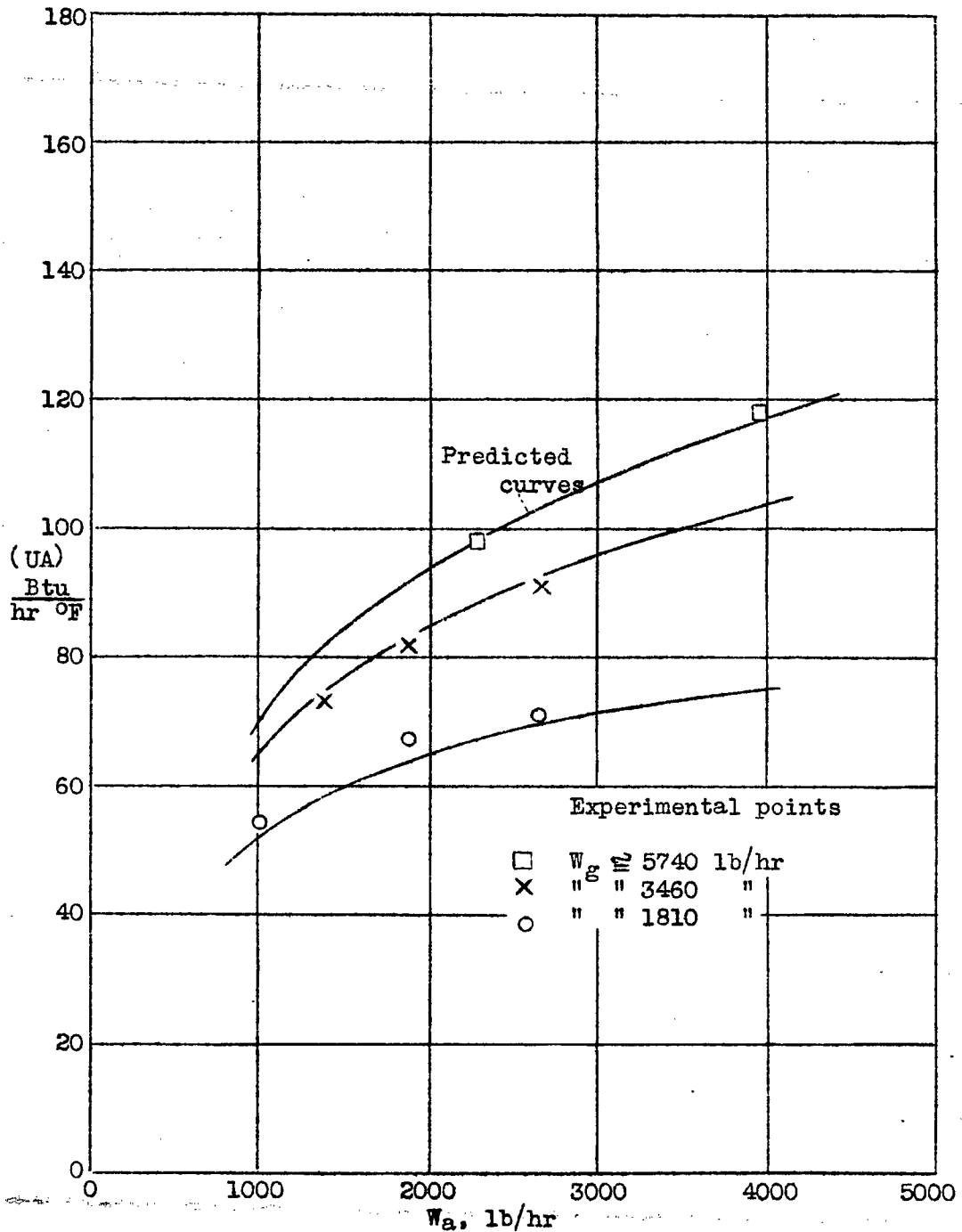


Figure 11.- Overall thermal conductance of the aluminum-alloy finned-type heater, using A-7 shroud, as a function of ventilating air rate.

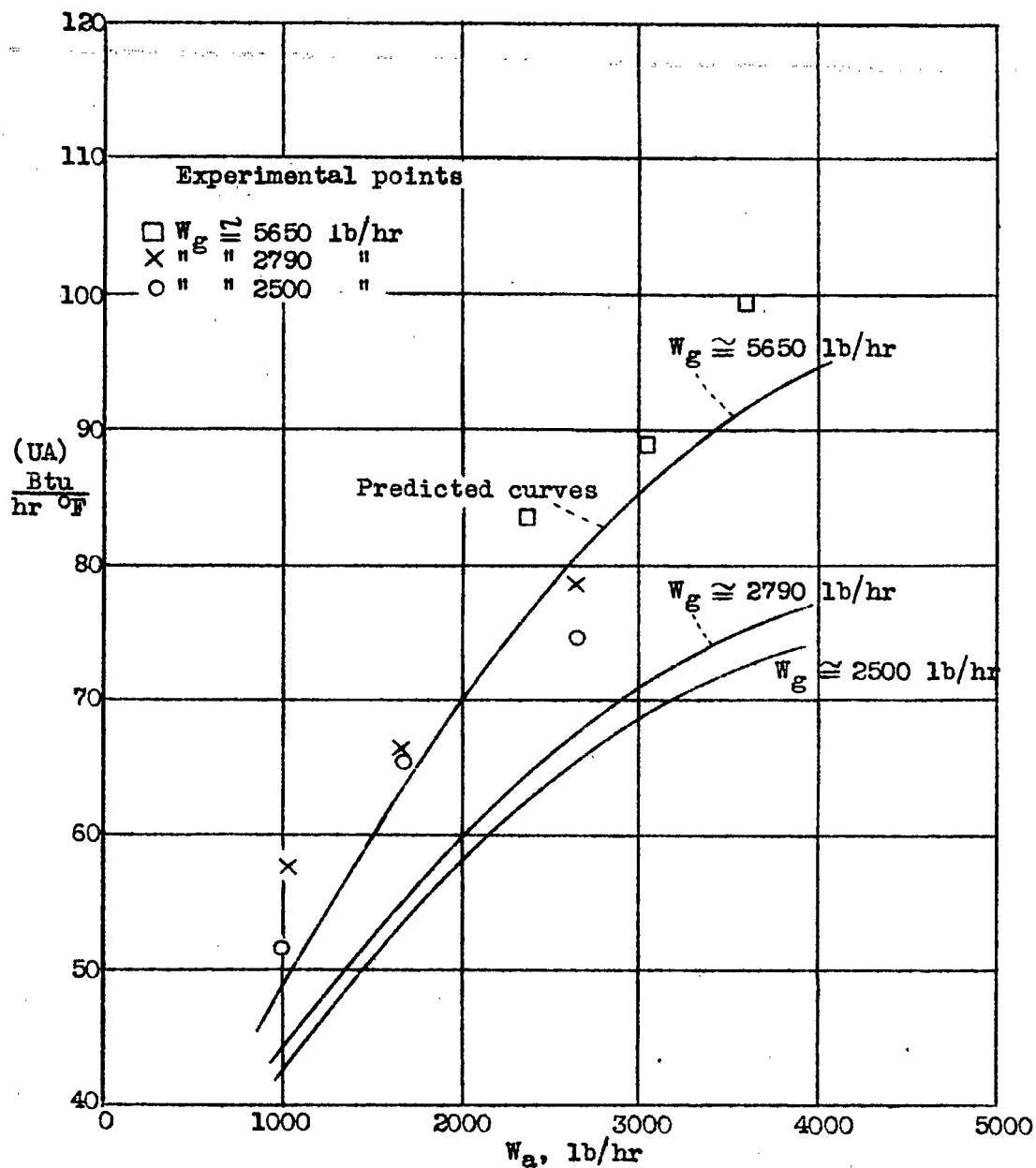


Figure 12.- Overall thermal conductance of the copper-stainless steel finned-type heater, using UC-1 shroud, as a function of ventilating air rate.

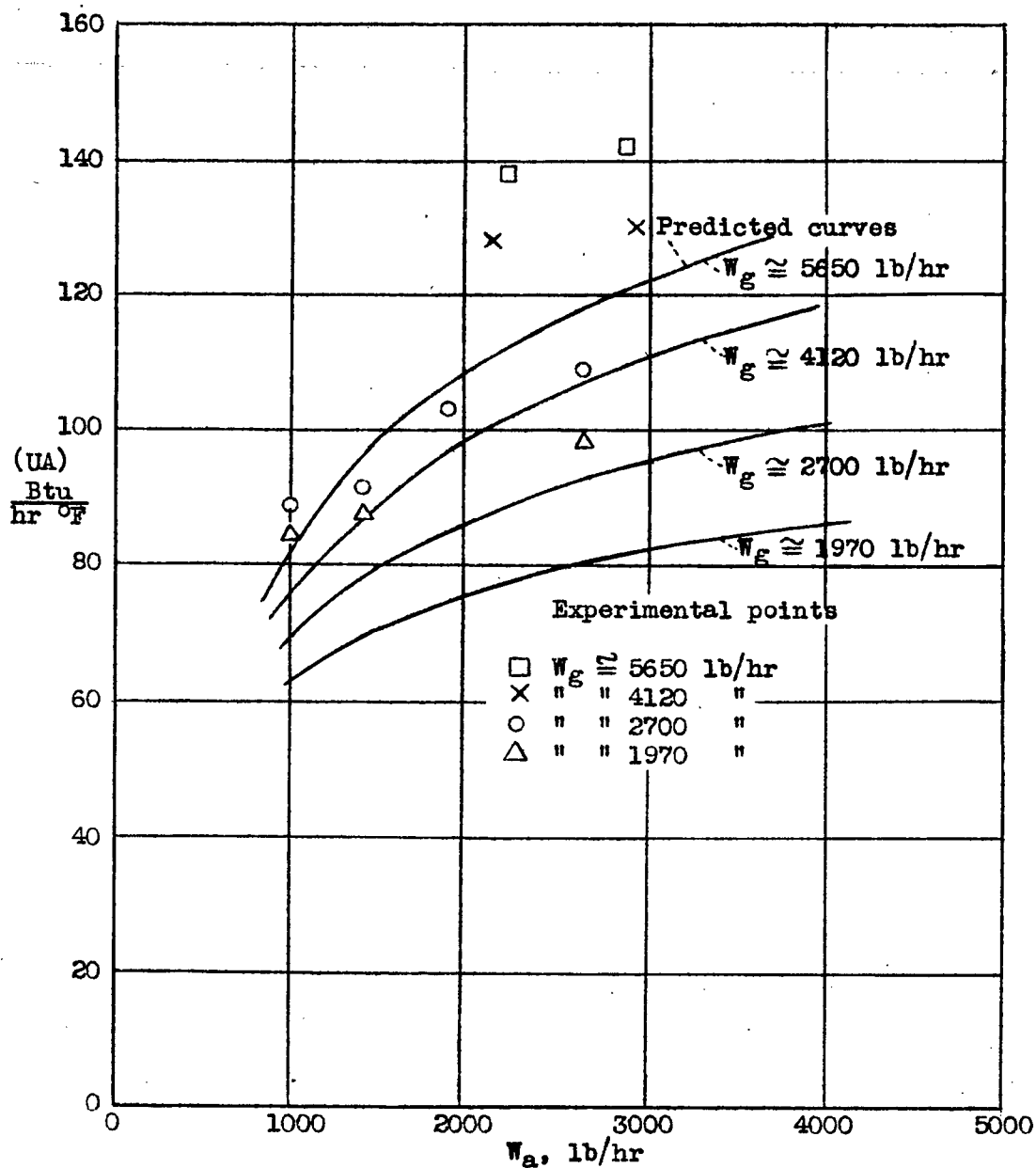


Figure 13.- Overall thermal conductance of the copper-stainless steel finned-type heater, using A-7 shroud, as a function of ventilating air rate.

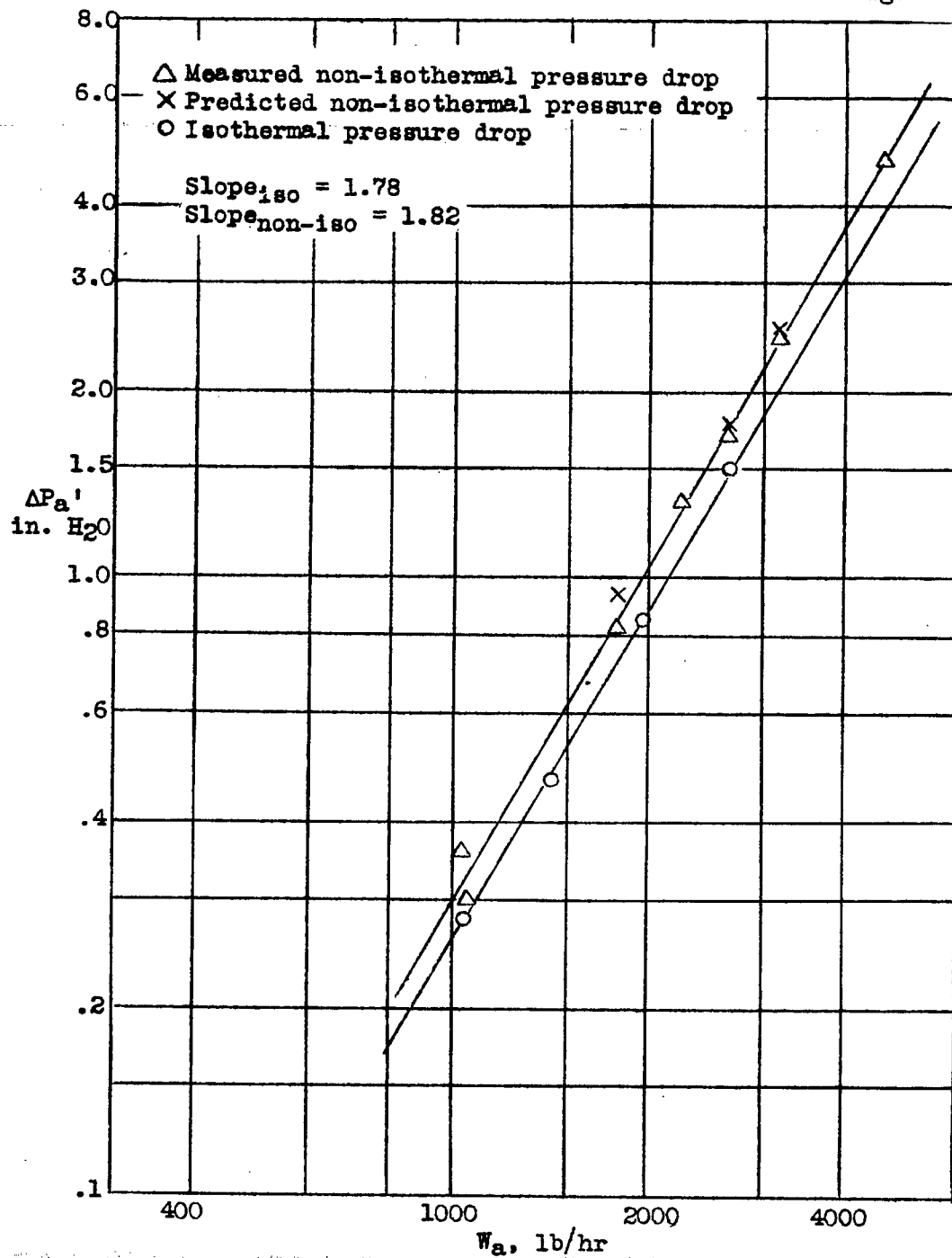


Figure 14.- Static pressure drop on the air side of the aluminum-alloy finned-type heater, using UC-1 schroud, as a function of ventilating air rate.

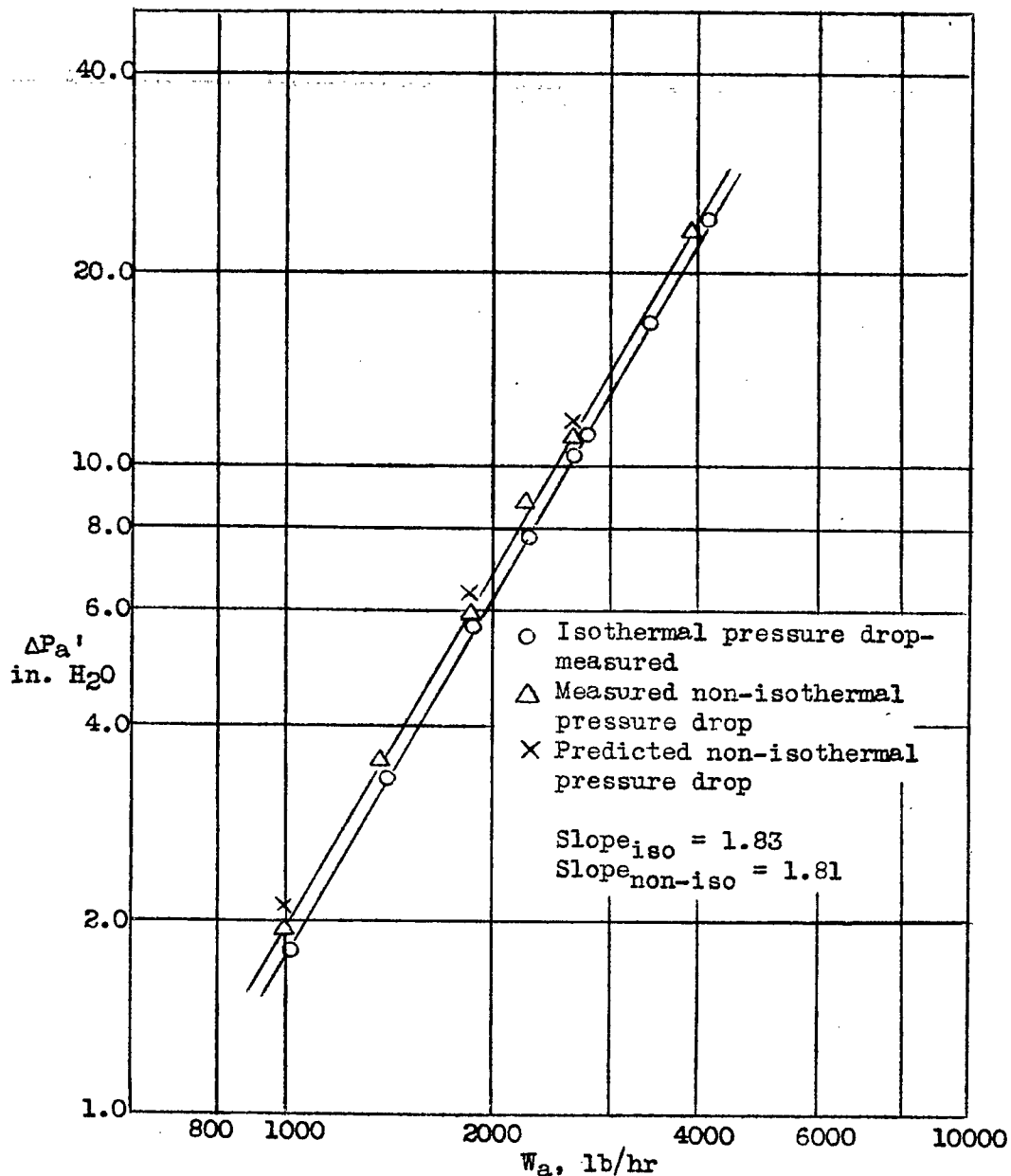


Figure 15.- Static pressure drop on the air side of the aluminum-alloy finned-type heater, using A-7 shroud, as a function of ventilating air rate.

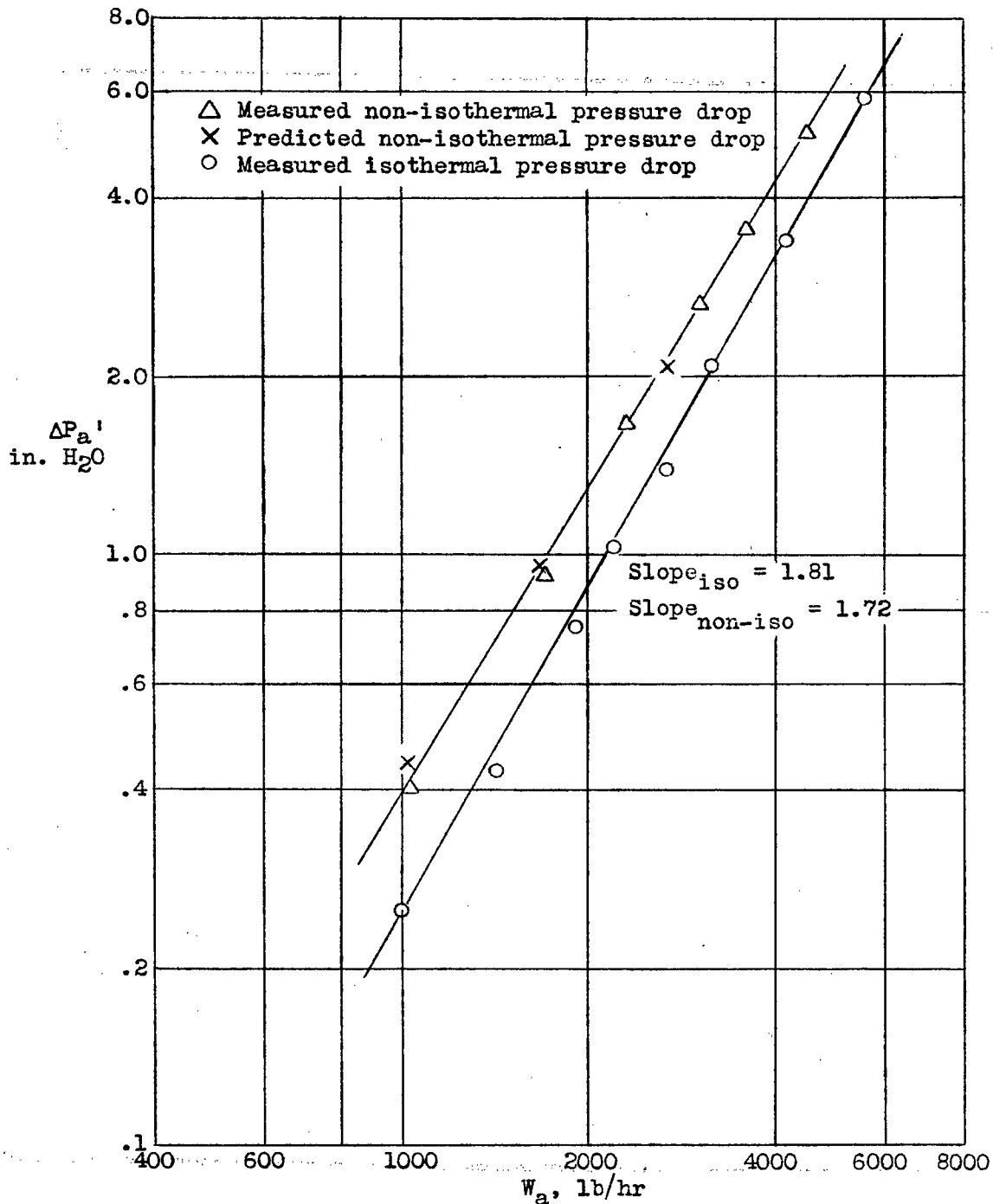


Figure 16.- Static pressure drop on the air side of the copper-stainless steel finned-type heater using UC-1 shroud, as a function of ventilating air rate.

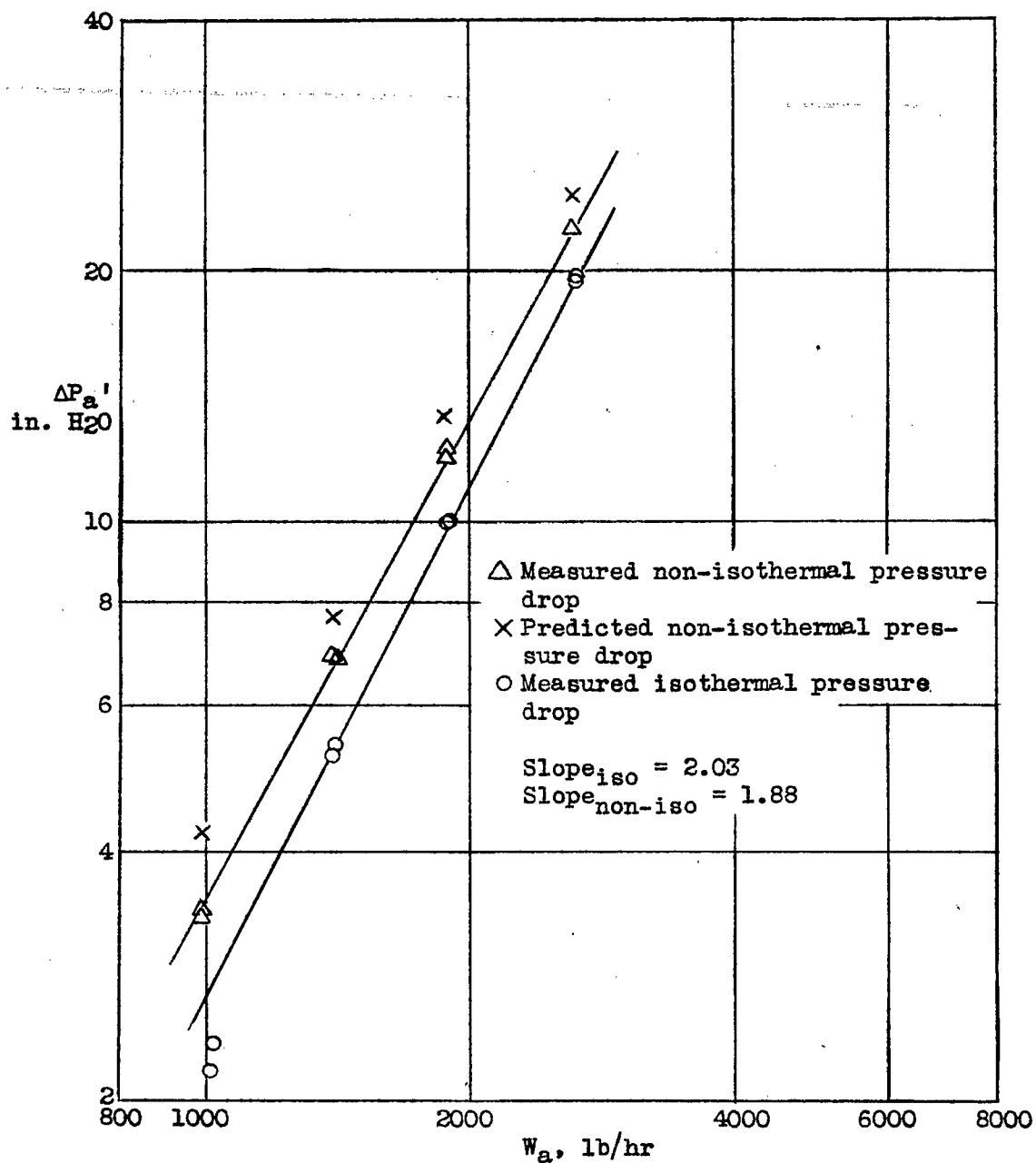


Figure 17.-- Static pressure drop on the air side of the copper-stainless steel finned-type heater, using A-7 shroud, as a function of ventilating air rate.

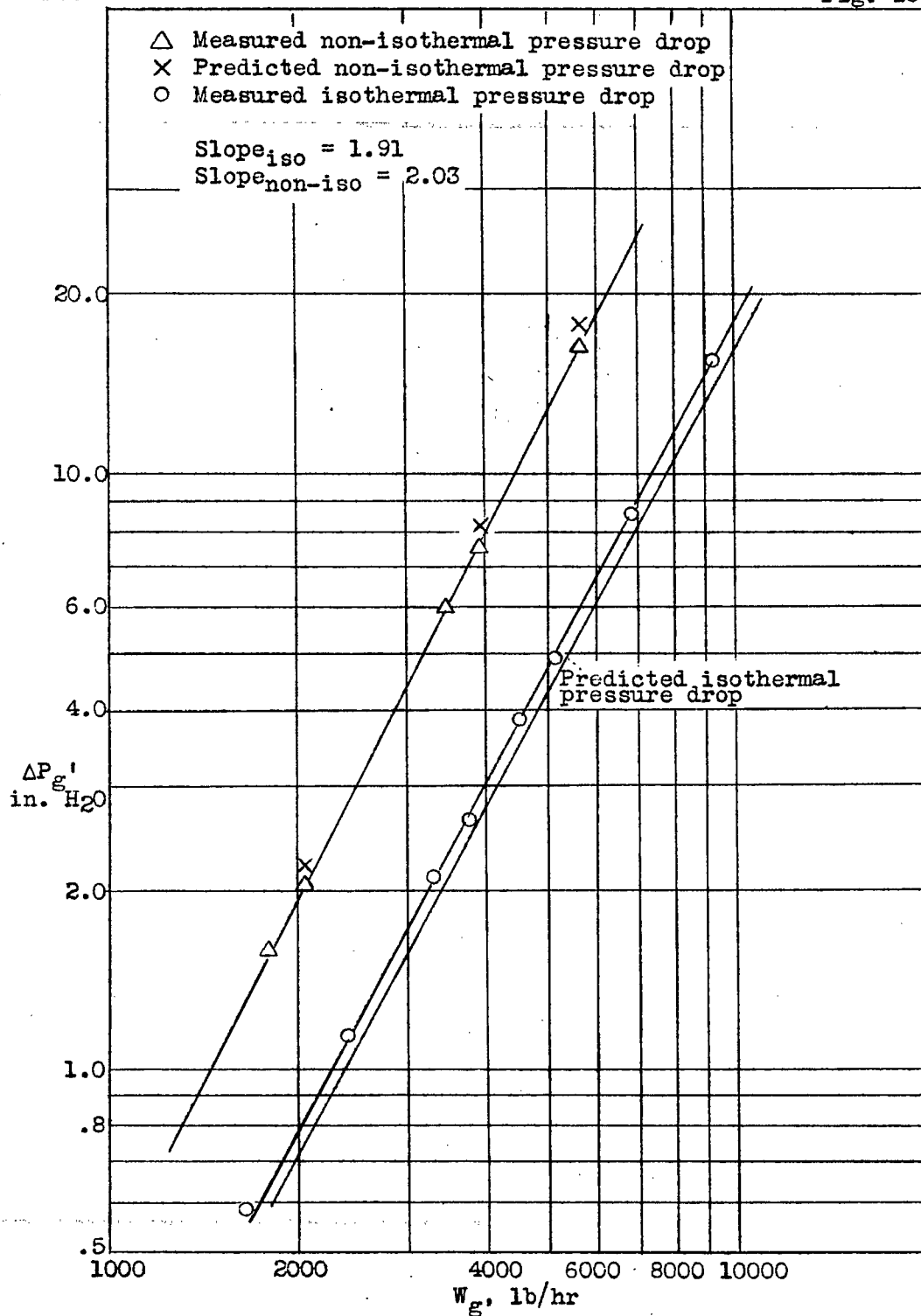


Figure 18.- Static pressure drop on the exhaust-gas side of the aluminum-alloy finned-type heater, as a function of the gas rate.

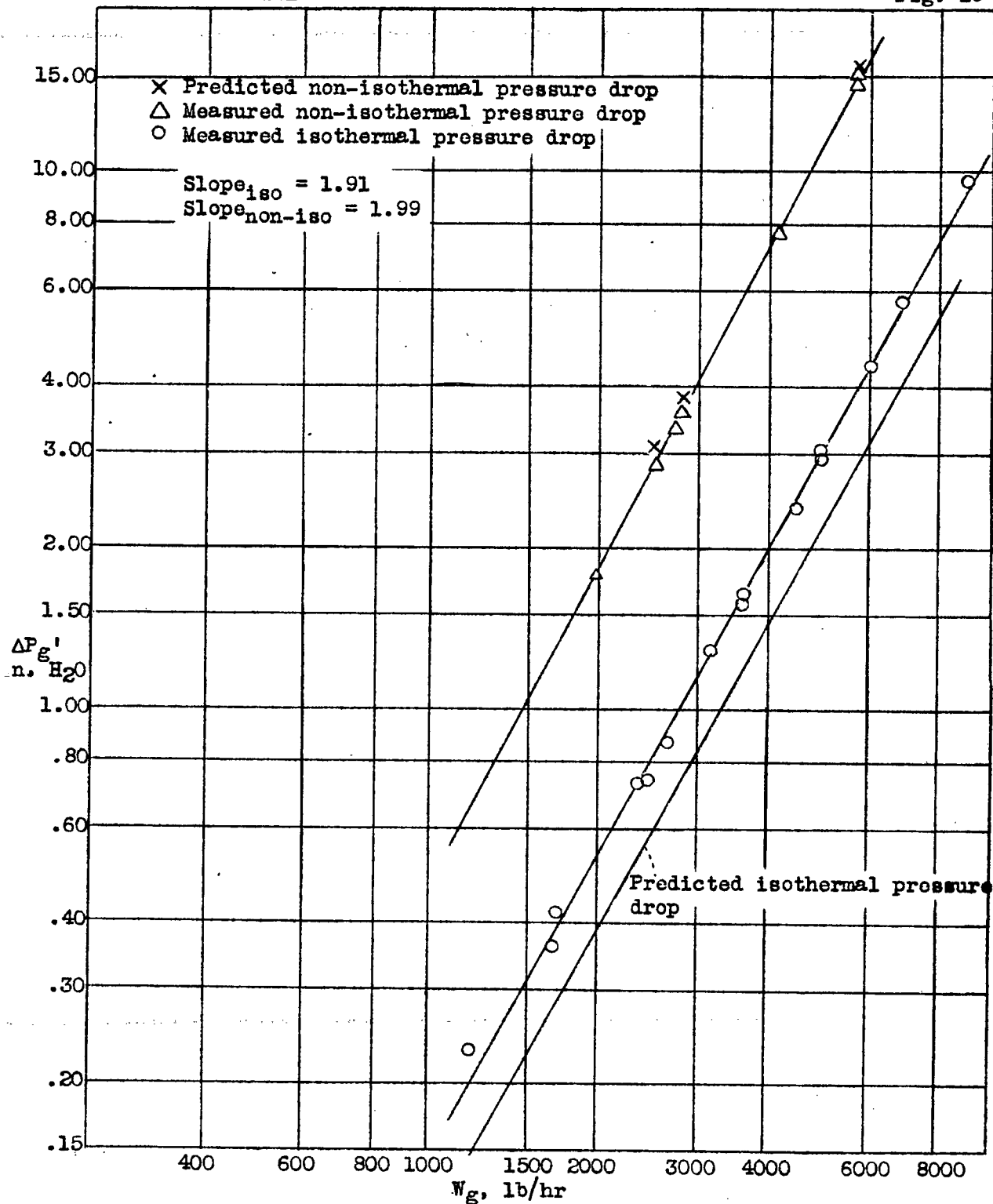
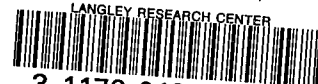


Figure 19.- Static pressure drop on the exhaust-gas side of the copper-stainless steel finned-type heater, as a function of the exhaust gas rate.

LANGLEY RESEARCH CENTER



3 1176 01354 4565